R-624

FINAL REPORT

APOLLO GAS-BEARING MATERIALS PROGRAM

by

Henry H. Rowe, Jr.

October 1968

INSTRUMENTATION LABORATORY

MASSACHUSETTS INSTITUTE OF TECHNOLOGY

Cambridge 39, Mass.

NASA CR 99539

R-624

FINAL REPORT

APOLLO GAS-BEARING MATERIALS PROGRAM

by

Henry H. Rowe, Jr.

October 1968

INSTRUMENTATION LABORATORY
MASSACHUSETTS INSTITUTE OF TECHNOLOGY
CAMBRIDGE, MASSACHUSETTS 02139

Approved: E. Hall
Associate Director

Approved: Ralph R. Ragan
Deputy Director

ACKNOWLEDGMENT

This report was prepared under DSR Project 55-24310, sponsored by the Manned Spacecraft Center of the National Aeronautics and Space Administration through Contract NAS 9-4576 with the Instrumentation Laboratory of Massachusetts Institute of Technology in Cambridge, Massachusetts.

R-624

FINAL REPORT

APOLLO GAS-BEARING MATERIALS PROGRAM

ABSTRACT

This report describes the results of a program to develop and evaluate an improved aluminum oxide ceramic gas-bearing material. The material for evaluation consisted of a fine-grain size, hot-pressed aluminum oxide, with and without a vapor-deposited coating of the same material. Evaluation included extended start-stop testing as well as slew testing to touchdown. Both material combinations exhibited superior wear characteristics to the conventional materials previously tested, but failed to provide a high-speed touchdown survivability for the design evaluated.

by Henry H. Rowe, Jr.

October 1968

TABLE OF CONTENTS

TABLE OF CONTENTS (Cont)

LIST OF ILLUSTRATIONS

LIST OF TABLES

CHAPTER I

BACKGROUND

Introduction

The results of the program for the development of a gas bearing for the Apollo I Inertial Reference Integrating Gyro[1] indicated that the ability of the gas-bearing material to withstand surface degradation during sliding contact was dependent upon microstructure (including grain size and porosity) and perfection of the surface finish. Characterization of the aluminum oxide materials which had been used for gas bearings showed that samples of the same nominal composition had considerable variation in chemical composition and rather inconsistent microstructures, including different pore sizes and pore contents, as well as variable and non-uniform grain size.

Wear studies showed that the resistance to attritive wear increased with the perfection of the surface finish; and that improved surface finish, hence improved wear resistance, could be obtained by vapor plating aluminum oxide on polycrystalline substrates to form a dense pore-free coating with minimal grain enlargement.

It was evident that improved gas-bearing life required the selection and control of the bearing material to a degree more rigid than was achievable with the current materials. Therefore it was decided to investigate the performance of a material in which more rigid control could be achieved: a fine-grained, hot-pressed aluminum oxide which would be of smaller, less-variable grain size than the cold-pressed and sintered materials presently specified, as well as being denser, hence freer from internal porosity, and of higher strength, thus less susceptible to crystal pull-out during grinding.

Table I presents a comparison of the physical properties of the fine-grained, hot-pressed material with those of the cold-pressed and sintered aluminas currently specified.

It was further decided to test a vapor-coated fine-grained alumina, as well as the hot-pressed material without coating, in order to evaluate both materials for performance in actual wheel assemblies.

Test Configurations

In order to evaluate these materials, both wear-test specimens and wheel assemblies were prepared. The wheel configuration chosen was that of the 18 IRIG Mod B, which is shown in Fig. 1.

The wear-test specimens consisted of journal sleeves made to the same configuration as the wheel journals.

The wear tests were run on the same wear-test apparatus used to evaluate the materials in the previous program.[1] In addition, the wear-test apparatus was modified so that additional wear testing could be done to simulate high-speed touchdown.

Table I

Physical properties of gas-bearing alumina ceramics.

	Greenfield AX-1	Lucalox	AVCO Hot Pressed Alumina
Composition	97 + % Al_2O_3	99.9% Al_2O_3	98.5% Al_2O_3
Grain Size (microns)	20-30	30-40	1-3
Compressive Strength (psi)	300,000	300,000	300,000
Ultimate Tensile Strength (psi)	10-20,000	20,000	75,000
Poisson's Ratio	0.25	0.205	0.2-0.3
Density (gm/cm^3)	3.86	3.96	3.96-3.98
Ultimate Transverse Rupture Strength (psi)	56,000	45,000	60,000
Coefficient Expansion $\left(in/in/^oF \times 10^{-6}\right)$	3.3	3.7	3.4

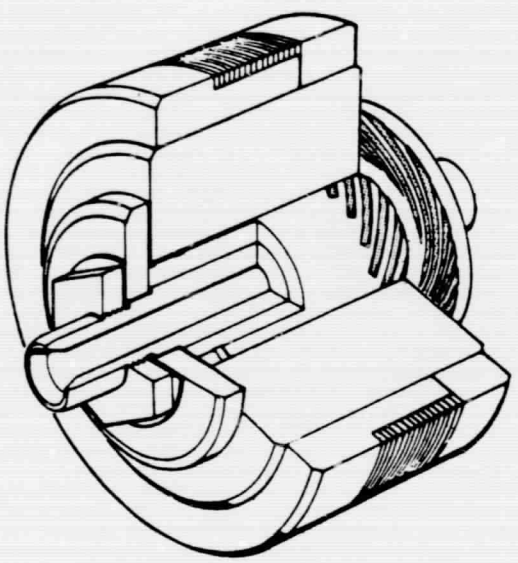

Fig. 1 18 IRIG Mod B gas-bearing wheel assembly.

CHAPTER II

MATERIALS DEVELOPMENT AND EVALUATION

In order to obtain the best possible material for evaluation in this program, as well as to maintain rigid control over the material specifications, a subcontract was placed with Lexington Laboratories, Inc., of Cambridge, Mass. It prepared specimens of fine grain size hot-pressed aluminum oxide, with and without vapor coating of the same material; performed material characterization and wear studies on these specimens; and supplied blanks of each of the aforementioned materials from which gas bearing assemblies could be fabricated.

Lexington Laboratories was chosen because of its experience in running wear tests in the previous program,[1] and their unique ability to apply the aluminum oxide coatings by the chemical vapor reaction and deposition technique.

Lexington Laboratories, Inc., in turn worked with the ceramics department of AVCO Corporation, Space Systems Division, Lowell, Mass., as the source for a near-theoretical density, small-grained, high-strength aluminum oxide. AVCO, by means of vacuum hot-pressing techniques, has produced an alumina with an as-pressed grain size of approximately 1 to 2 microns; this being 20 to 30 times smaller than the available cold-pressed aluminas, and 3 to 5 times smaller than most other hot-pressed aluminas.

The fine-grained alumina results in a better surface finish since pull-outs, which are the major source of surface porosity, are of correspondingly smaller size than those in larger-grained materials. Also, less pull-outs occur during machining since the bonding of the cyrstals is much stronger in the AVCO material, as shown by its high tensile strength as compared to the other aluminas.

The Lexington Laboratories' chemical-vapor deposition technique was used to deposit an epitaxial layer of aluminum oxide on half of the material supplied, using the AVCO alumina as the substrate material so as to obtain the high-purity, high-perfection crystalline surfaces such as were realized in the previous program with vapor-deposited crystals of fine grain size. As had been demonstrated before, this technique can deposit a layer of several mils thickness which is free from such surface defects as voids and cracks and which reproduce the grain structure of the substrate material. In addition, this technique also gave surfaces with excellent wear characteristics.

These two materials (the AVCO vacuum hot-pressed alumina and the Lexington Laboratories vapor-coated alumina) then formed the bases for evaluation in this program. The results of the materials development and evaluation are contained in Lexington Laboratories' final report on subcontract 349 which is included as Appendix I of this report.

Surface-finish measurements and photomicrographs of the finish-lapped AVCO hot-pressed alumina test sleeve and the vapor-coated AVCO test sleeve are shown in Fig. 2a and 2b. Figure 2c shows a typical lapped gas-bearing surface of the cold-pressed and sintered alumina material. From these figures it can be seen that the surface finishes attainable with the hot-pressed alumina, both with and without a vapor-deposited coating, are far superior to those obtained using the materials presently specified for gas bearings.

It was noted from the photomicrograph of the vapor-coated specimen that some surface porosity did occur, possibly as the result of crystal pull-out during grinding and finishing operations. Some attempt was made to improve the finish by additional lapping. However, only a limited amount of material was removed for fear of removing the plated surface. It is felt that better surfaces may be achieved by removing less stock through grinding and leaving more material for removal by lapping.

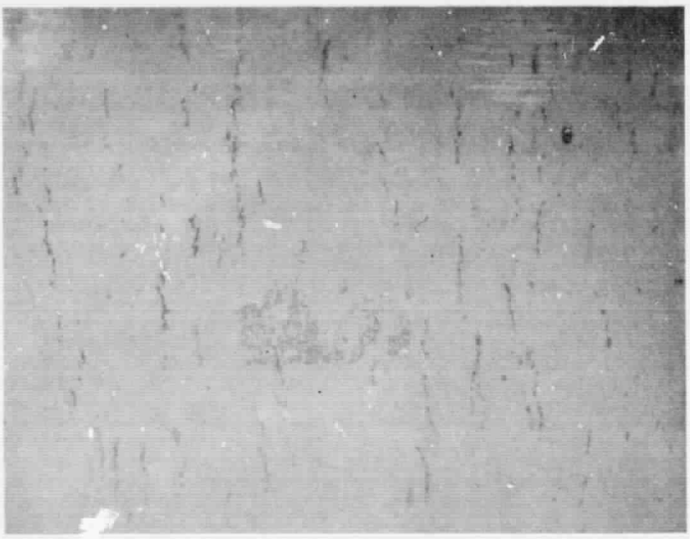

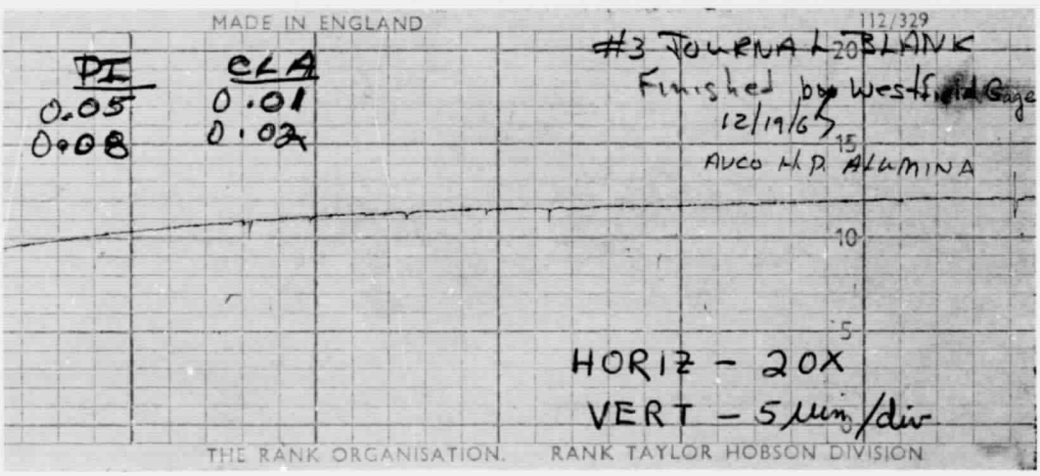

Fig. 2a Photomicrograph (100 X) and Talysurf surface finish trace on AVCO hot pressed alumina test journal.

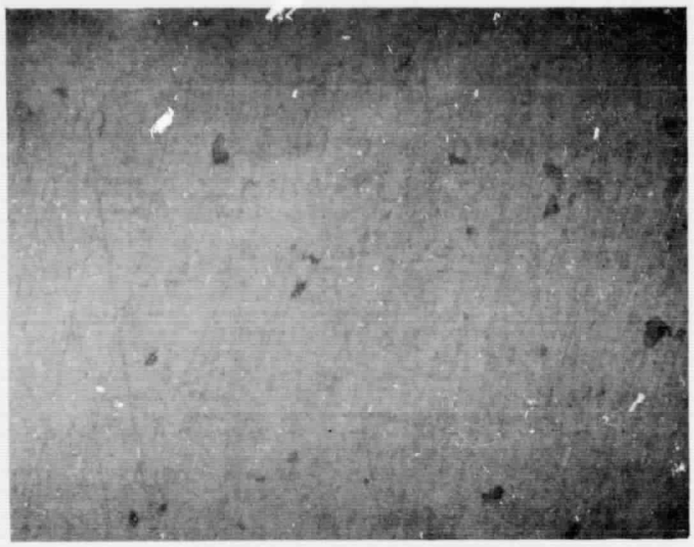

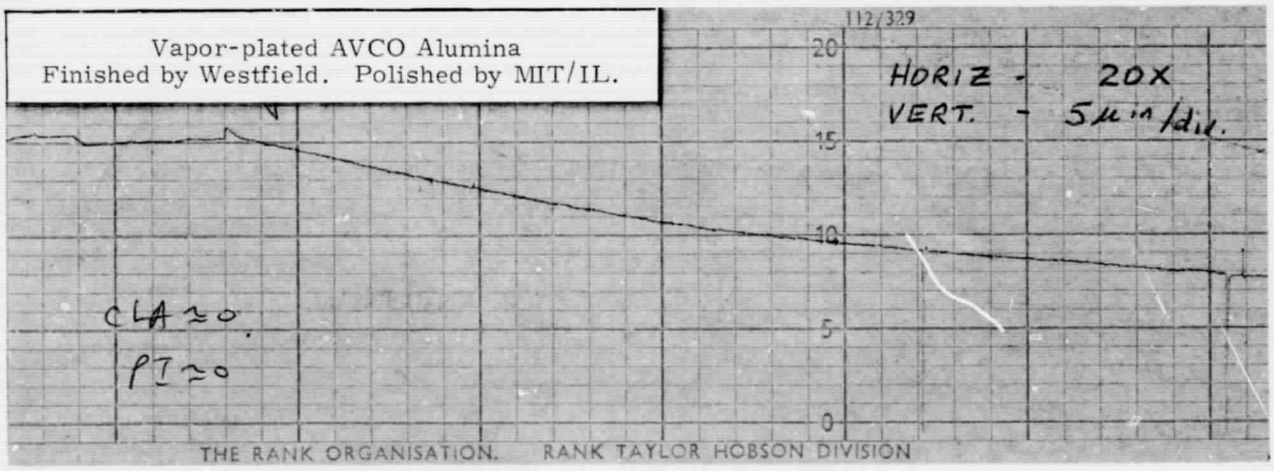

Fig. 2b Photomicrograph (100 X) and Talysurf surface finish trace on vapor coated AVCO hot pressed alumina test journal.

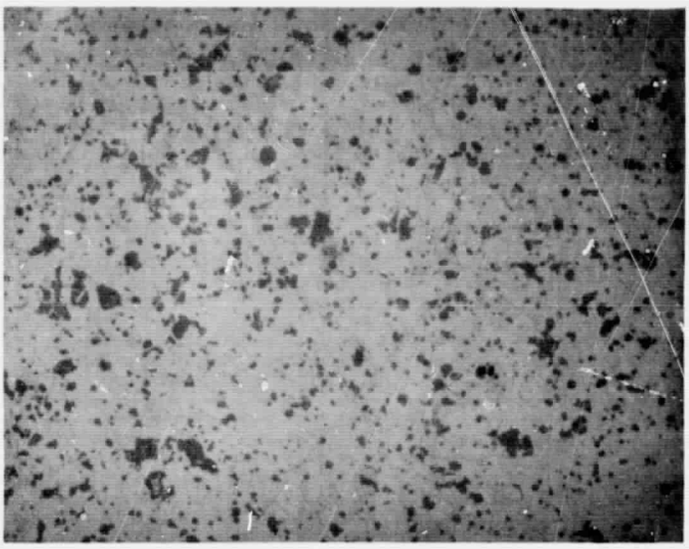

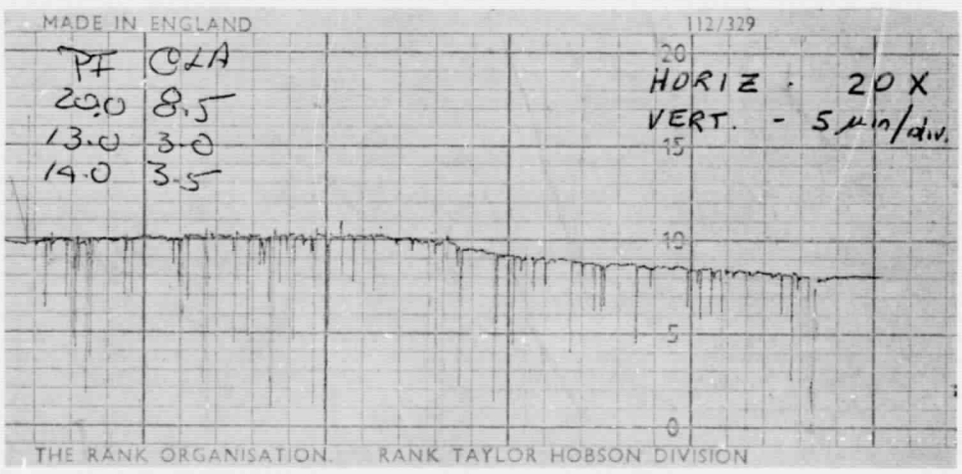

Fig. 2c Photomicrograph (100 X) and Talysurf surface finish trace on typical finish lapped gas bearing ceramic surface (AX-1 alumina).

CHAPTER III

WHEEL FABRICATION AND ASSEMBLY

Fabrication

Eight sets of blanks, four each of the two test materials from which the gas-bearing assemblies were to be fabricated, were supplied by Lexington Laboratories, Inc. Each set consisted of a hub blank, a journal sleeve blank, and two end cap blanks. The balance of the wheel hardware was procured from commercial sources and the piece parts were assembled and bearing surfaces finished at the MIT Instrumentation Laboratory.

It was decided to do the finish machining, grinding and lapping of the ceramic materials at the MIT/IL machine shop so as to gain experience and knowledge of the machining characteristics of the AVCO and plated-alumina ceramics as compared to the other ceramics which had been used. It was found that the AVCO hot-pressed alumina reached a finished surface much faster than the cold-pressed materials. This was to be expected; because of the fine grain size, less material must be removed in order to get below any layer damaged by crystal pull-out from previous grinding operations.

Also, because of the high strength of the AVCO alumina, it was less susceptible to crystal pull-out from grinding operations, and finish-lapped surfaces could be achieved which were virtually free from surface voids.

For the vapor-plated parts, blanks of the AVCO alumina were first machined two to three mils under the desired finished dimensions on the bearing surfaces and returned to Lexington Laboratories for the chemical vapor-deposition process. Following vapor coating, however, it was found that the hub blanks had grown by approximately one percent as a result of thermal growth of the alumina when heated to 1700^{o} C so that all of the vapor plating would have been removed in finish machining. Hence these blanks were returned to Lexington Laboratories for re-machining to the pre-plate dimensions and replating. Two hub blanks were recoated. However, the other two hub blanks were found to have surface defects on critical bearing surfaces following machining, and it was decided to replace these blanks with new ones.

In order to overcome the thermal growth problem, these two replacement blanks were first pre-heat-treated at the plating temperature, then ground to pre-plate dimensions and plated.

It was also found necessary to replate the four journal sleeves on the ends to compensate for their being too short initially to match the finish-plated hubs to give the proper end shake.

In addition, it was found that three of the plated end caps broke through the plated surfaces during lapping; therefore these pieces were also returned for additional plating.

It is of interest to note that, while the fine-grained vacuum hot-pressed alumina is characteristically gray in color (due to direct carbon pickup from the molds and/or diffusion of the reducing atmosphere (CO and CO_2) into the alumina during hot pressing[2]), during the chemical vapor deposition process the carbon component is driven off leaving the plated blanks basically white in color.

Wheel Assembly

A total of eight sets of wheel parts were fabricated in this program and, while the contract required a minimum of only six assemblies to be built, a total of eight wheels were assembled and tested. Four wheels were of the AVCO hot-pressed alumina, unplated, and four had bearing surfaces of vapor-deposited aluminum oxide on the AVCO material as a substrate.

Following a standard evaluation program in which all of the wheels were subjected to power measurements, vibration tests, and start-stop testing; several of the assemblies were subjected to an extended evaluation program.

Disposition of the wheel assemblies was as follows:

Unplated Alumina Assemblies

Wheel 18 BM-1

Accidental touchdown suffered on slew testing. Cleaned up and run on extended start-stop tests.

Wheel 18 BM-2

Initially a spare assembly. Wheel was assembled and underwent standard evaluation. Stationary components subsequently used in assembly of prototype wheel for 18 IRIG Mod B 0420 series instruments or evaluation of cooldown stability improvement.

Wheel 18 BM-3

Used on extended evaluation test program. Slew-tested to touchdown.

Wheel 18 BM-4

Used on extended evaluation test program for extended start-stop testing. Delivered to NASA/MSC in float assembly.

Vapor Plated Alumina Assemblies

Wheel 18 BM-5

Initially a spare assembly. Assembled and run on extended start-stop evaluation.

Wheel 18 BM-6

Used on extended start-stop evaluation tests.

Wheel 18 BM-7

Used on extended evaluation test program. Slew-tested to touchdown. Also used for extended start-stop tests.

Wheel 18 BM-8

Delivered in float assembly to NASA/MSC.

CHAPTER IV

STANDARD GAS-BEARING EVALUATION PROGRAM

Gas-Bearing Evaluation

All of the gas-bearing wheels were subjected to a standard evaluation program consisting of wheel power measurements, one g-RMS sinusoidal vibration between 20 and 4000 Hz to determine the axial and radial resonant frequencies and bearing compliances, and a series of 1000 start-stop cycles in each of the three principal positions: +SRA down, -SRA down, and SRA horizontal.

Then, in order to evaluate the bearing materials and to gain a comparison with the previous materials used, several of the assemblies were subjected to an extended evaluation program consisting of an extended start-stop life test and a slew-rate capability determination which included slewing to touchdown in order to ascertain touchdown survivability.

The results of these tests are reported in the following sections.

Standard Wheel Evaluation Program

Power Measurements

Power measurements were made on each assembly to determine minimum breakaway voltage, minimum synchronous voltage and power, and total wheel power when running in sync at the nominal running voltage of 28 volts/phase.

These measurements, together with average values for standard 18 IRIG Mod B units, are presented in Table II.

Vibration Measurements

All of the wheel assemblies were subjected to 1-g RMS sinusoidal vibration along both the thrust and journal axes over a frequency range of 20 to 4000 Hz to determine the bearing axial and radial resonant frequencies and the bearing compliances. Fig. 3 shows a typical vibration response curve along the two axes. Table III summarizes the axial and radial resonant frequencies and compliances for the eight wheel assemblies measured in this program, together with an average of these values for a standard 18 IRIG Mod B assembly.

Start-Stop Testing

Each of the wheel assemblies was subjected to the standard start-stop test sequence as a part of the general wheel qualification. This testing sequence consists of running the wheel for a total of 3000 start-stop cycles, 1000 in each of the three principal positions; +SRA down, -SRA down, and SRA horizontal. The wheel supply voltage is set at 25 volts/phase, 3 volts below the standard systems operating voltage; and any failure of the wheel to start at this voltage level constitutes a failure to pass the test even though the wheel may start following a subsequent application of the starting voltage with the wheel in the same test orientation.

This criterion for failure was also used in running the extended start-stop tests reported in the next section.

All of the wheel assemblies successfully passed the standard start-stop test.

Slew-Rate Test

In addition to the aforementioned qualification tests, each wheel assembly was subjected to a slew-rate test to verify that the design would pass the minimum slew-rate requirement of five radians per second, both clockwise and counterclockwise. Again, all of the assemblies qualified.

Table II
18 IRIG Mod B Gas Bearing
Wheel Power Measurements
1 atmosphere of neon @ 130°F
(All measurements with standard test stator in fixture unless noted otherwise)

Wheel	Wheel Power (Watts) @ 28 V/ϕ	Minimum Synchronous Voltage, V/ϕ	Minimum Breakaway Voltage		
			SRA Horizontal	+SRA Down	-SRA Down
18 BM - 1	3.92	19.2	14.5	15.8	14.9
18 BM - 2	3.87	18.7	15.5	17.2	16.5
18 BM - 3	3.83	19.6	17.3	20.0	19.8
18 BM - 4	4.27	19.3	15.0	19.0	15.6
	5.52*	20.9*	15.5*	16.8*	17.5*
18 BM - 5	3.90	21.0	14.0	14.0	14.0
18 BM - 6	4.02	20.9	15.0	15.5	16.0
18 BM - 7	4.02	19.5	14.0	14.5	14.5
18 BM - 8	4.43	21.5	13.5	14.2	13.5
	5.23*	21.0	14.5	20.5	17.0
Typical 18 IRIG Mod B	3.84	18.8	14.2	16.7	16.9
	5.15*	20.4*	15.0*	17.1*	17.5*

* measured in float assembly

Table III
Axial & Radial Resonant Frequencies and Compliances

	Resonant Frequency (Hz)		Compliance (μ in/lb)	
Wheel	Axial	Radial	Axial	Radial
18BM-1	2850	3017	7.3	6.9
18BM-2	2445	3011	17.3	7.6
18BM-3	2500	3120	16.3	8.0
18BM-4	3220	3330	8.0	5.5
18BM-5	2425	2808	22.2	8.3
18BM-6	2450	3160	16.5	8.2
18BM-7	2245	3000	15.3	6.7
18BM-8	2548	2928	20.2	8.3
AVERAGE 18BM	2583	3047	15.4	7.4
Typical 18 IRIG MOD B	2276	2940	20.3	7.7

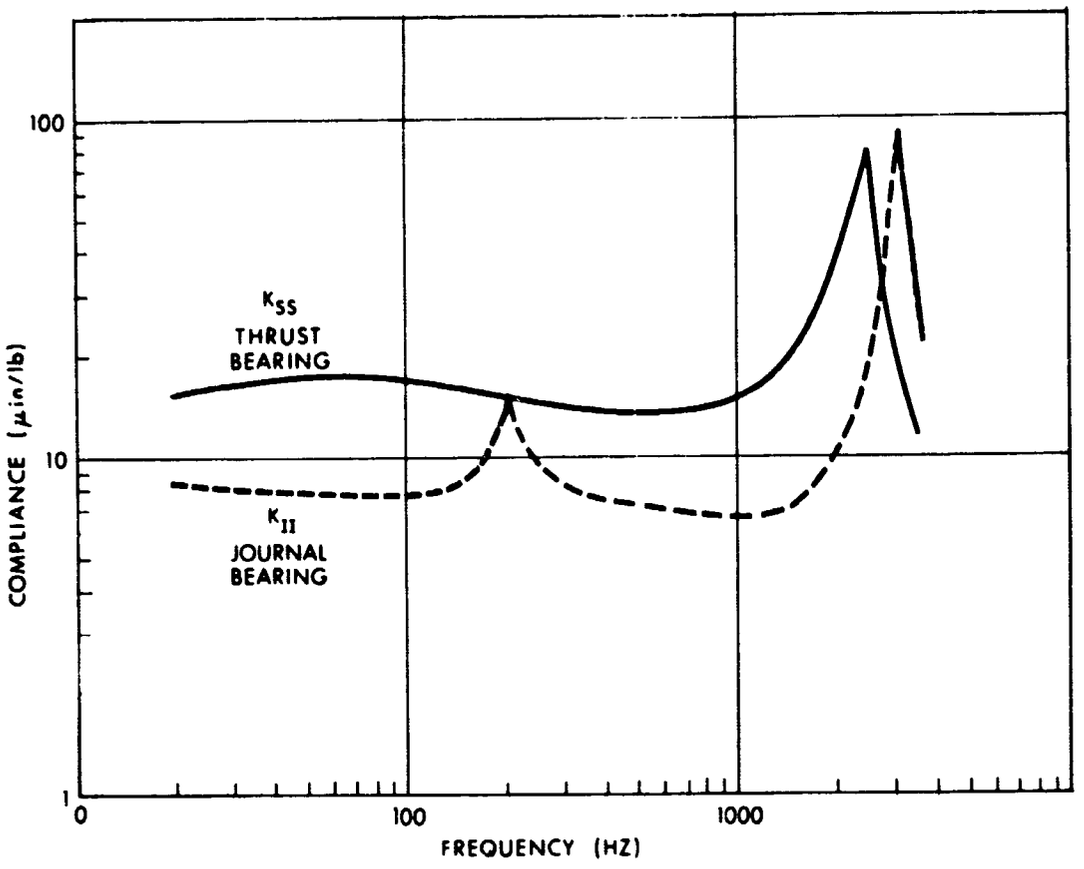

Fig. 3 Typical gas-bearing vibration response curves (wheel 18 BM-3).

CHAPTER V

EXTENDED EVALUATION PROGRAM

Extended Start-Stop Testing

Following qualification of the wheels and having completed the standard wheel evaluation tests, two of the wheel assemblies (one assembly of each material configuration) were scheduled for extended start-stop testing to determine the relative start-stop capabilities of the two material combinations and to determine what advantage, if any, these materials might possess over the previous materials used.

Start-stop testing was done in the manner described in the previous section, with the first failure to start upon application of 25 volts per phase constituting a test failure. However, instead of halting the testing in any one positional mode at a specific number of start-stop cycles, testing continued in that mode until the failure criterion was reached. Then the assembly was moved to the next test mode and the testing resumed with no attempt to clean the assembly between failures.

The two wheel assemblies selected for this evaluation were wheel 18BM-4 (AVCO alumina, unplated) and wheel 18BM-6 (vapor-plated alumina).

The results of testing these two assemblies led to a desire to obtain additional start-stop data. Therefore, both wheels were reassembled for additional start-stop testing and, in addition, one more unplated assembly and two more plated assemblies were included in this phase of the evaluation.

The results of the extended start-stop tests are presented in the following table:

Table IV

Extended start-stop test results.

		No. of Start-Stop Cycles to First Failure		
Material	Wheel	+ SRA Down	- SRA Down	SRA Horizontal
AVCO Hot Pressed Alumina	18 BM-4	14,050	13,470	3646
	18 BM-4[A]	-	-	Terminated at 100,000[1]
	18 BM-1	26,619	8441	35,454
Vapor Plated Alumina on AVCO HP Alumina	18 BM-6	3412	119,814	Not Run[2]
	18 BM-6[A]	8500	-	16,076[3]
	18 BM-5	80,450[3]	-	-
	18 BM-7[4]	2659	3575	-
AX-1 Alumina	Typical	4200	5500	> 30,000
Vapor Plated AX-1 run vs. Unplated AX-1	Special	4550	2504	-

[1]Repeat SRA Horizontal Run following teardown and cleaning after first extended Start-Stop test assembly.

[2]SRA Horizontal Run was not made so that the wheel could be examined to determine cause for gross difference in Start-Stop performance between the two ends.

[3]Wheel still running in this position at the time report was written.

[4]Start-stop tests run after wheel had been slew-tested to touchdown.

It should be noted that the testing sequence was in the order given, i.e., +SRA down, -SRA down, then SRA horizontal.

It should also be noted that all start-stop test results are for assemblies which have been microlubricated with sodium stearate, following the procedures specified in Appendix II.

Also included in the table for comparison are typical values for standard assemblies made from AX-1 alumina as well as the results of running a set of vapor-plated AX-1 end caps against an unplated AX-1 rotor in a standard assembly.

From the results tabulated above, it can be seen that AVCO hot-pressed alumina gives three to five times the start-stop capability of the standard materials, while the vapor-plated alumina on the AVCO hot-pressed substrate has the potential of extending the start-stop capability twenty-fold.

The results of running the vapor-coated AX-1 against the unplated AX-1 were disappointing. However, it is quite possible that the unplated member was the limiting factor and the results might have been better if both bearing surfaces had been vapor-coated.

Slew-Rate Capability Determination

The gas bearing had been designed to meet a minimum slew-rate requirement of five radians per second, and all of the assemblies were tested to this level. It was the purpose of this portion of the task effort to determine the actual rate capability of the design and, since this would involve slewing to touchdown, also to determine the ability of the bearing to survive a high-speed touchdown. Two wheel assemblies were to be entered into this evaluation.

Background

In order to determine the slew capability of the wheel without slewing to touchdown, the conventional method of testing is mounting the wheel in a fixture, SRA horizontal, on a Genisco Rate-of-Turn Table and gradually increasing the table rotational rate, monitoring total wheel power all the while, until a sharp increase in the wheel power level is detected. This point constitutes the maximum rate which the wheel can sustain without touching down and is usually within approximately 10 per cent of the actual bottoming slew rate.

This method of testing, however, is not without serious drawbacks. First, of course, there is always the danger that the testing will not be stopped in time and that the wheel will touch down. Also, the determination of the point at which to stop the test is subject to the discretion of the technician running the test, making the choice of the test-termination point a nebulous one. And thirdly, fluctuations in line voltage can cause extraneous power changes, further clouding the measurements.

Therefore it is desirable to find another method of determining the slew-rate capability that presents less danger to the wheel and yields more positive results.

One method which suggests itself is using capacitance probes to measure actual rotor displacements (as is done during sinusoidal linear-vibration testing) rather than relying on monitoring wheel power. This cannot be done conveniently on a rate-of-turn table because of the inability to read the probe output signals through the slipring noise levels.

Therefore, an alternate approach in which capacitance probes can be utilized to measure the rotor displacements, is the use of an angular vibrator.

Discription of Angular Vibration Tests

In running the angular vibration tests to determine the slew rate capacity of a gas-bearing assembly, an MB Model CA 1050 Torsional Calibrator was used. This unit is capable of producing torsional oscillations between 20 and 1900 Hz with a maximum torsion displacement of 45^{o} total between mechanical stops.

A signal generator attached directly to the table monitors angular velocity of the table motion and these outputs are read directly on an angular velocity meter.

The wheel was mounted in the vibration fixture with SRA horizontal on the angular vibration table and four capacitance probes were used to measure the rotor displacement (Fig. 4). Probes #1 and #2 on the thrust face of the rotor, as well as probe #3 on the rotor OD, sense the motion of the rotor about the axis of excitation (i.e., the input axis). Probe #4 is at right angles to probe #3 and senses motion of rotor about an axis perpendicular to both the spin axis and axis of excitation (i.e., the output axis).

Holding the angular acceleration level constant at 1000 rad/sec^2, the wheel was vibrated at several discreet frequencies between 20 and 1900 Hz and the corresponding rotor displacements measured. From these measurements and a knowledge of the bearing geometry (i.e., bearing clearances and lengths), it is possible to calculate that angular velocity level at which all of the available bearing clearance would be used up (or the maximum slew-rate capability) assuming that the angular stiffness of the bearing is linear. These results are presented in Fig. 5 and 6.

In order to provide a further correlation between the angular shaker vibration test and the slew tests, a parallel set of angular vibration tests were run on the "MIT Precision Angular Vibrator". This is a two-axis mechanical shaker operating between frequencies of 7.5 and 119 Hz. For the purpose of this test, of course, only one axis of vibration was used. This machine is driven by a Reeves drive through a set of cams. Adjustments on the cams determine the amplitude of vibration about each axis, and the speed of the Reeves drive determines the frequency of vibration. Testing was done at discrete frequencies from 7.5 to 70 Hz. The test setup is shown in Fig. 7. The test results are shown in Fig. 5 and 6.

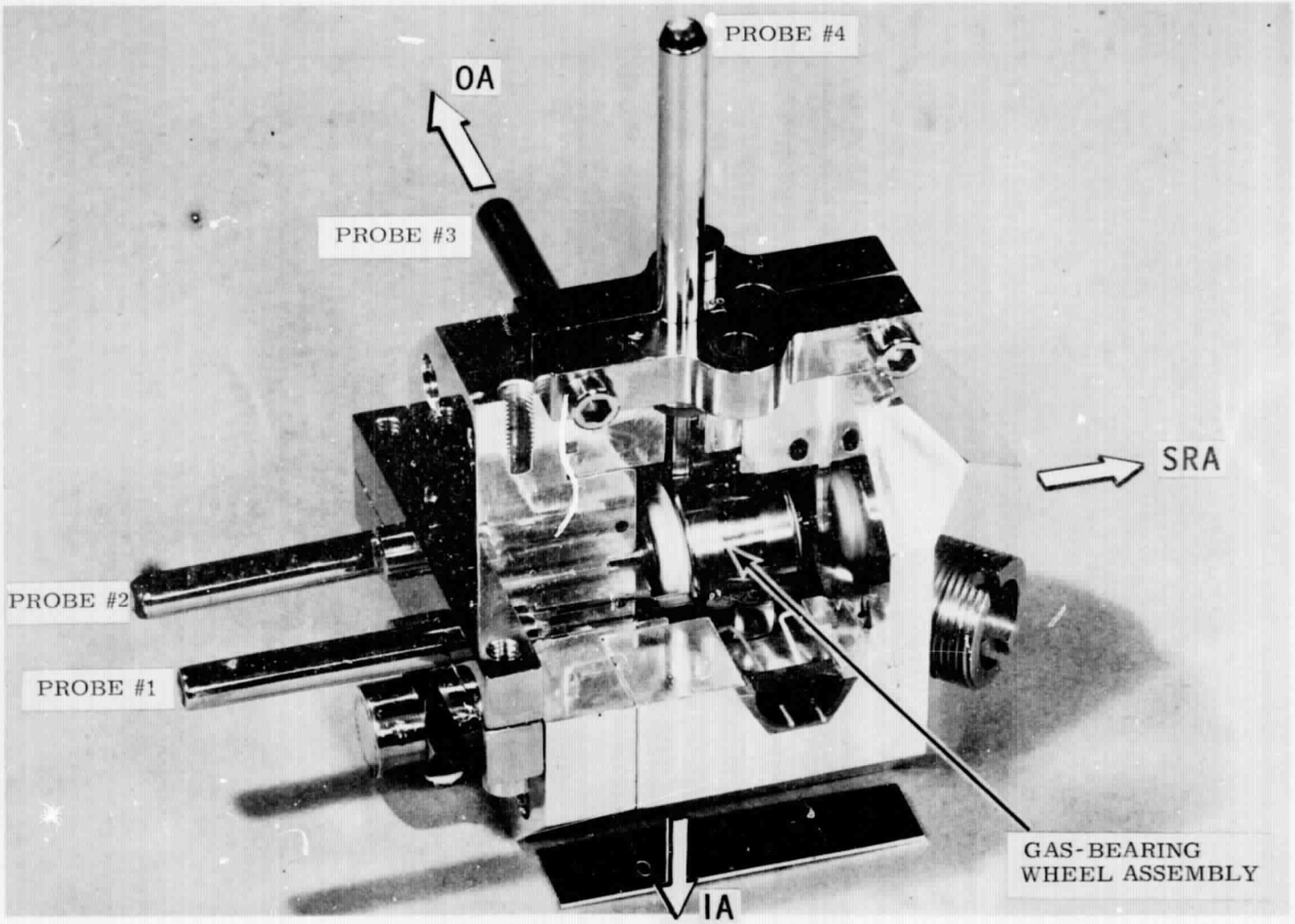

Fig. 4 Vibration fixture and capacitance probes for angular vibration tests (cutaway view).

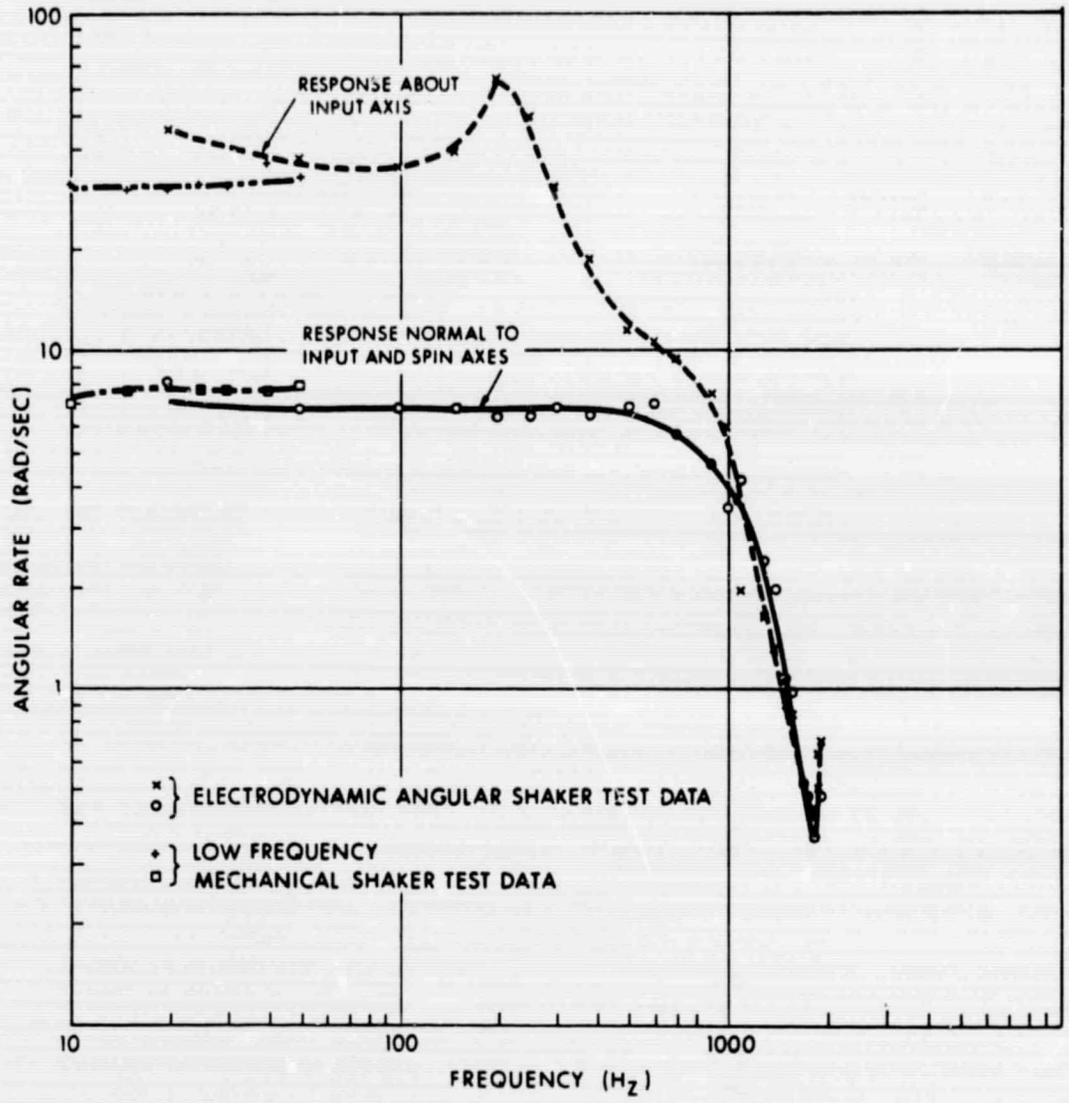

Fig. 5 Angular vibration capability of wheel 18 BM-3.

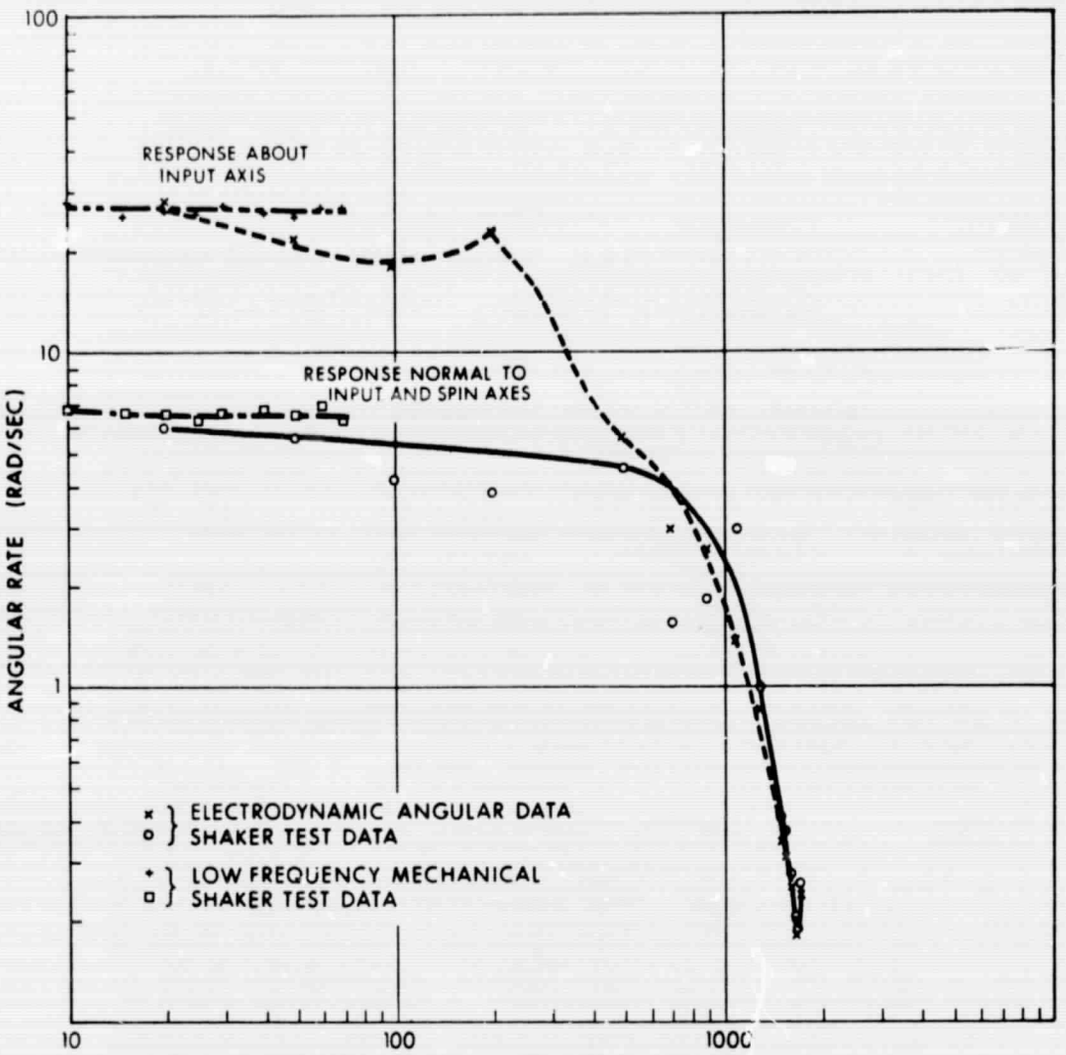

Fig. 6 Angular vibration capability of wheel 18BM-7.

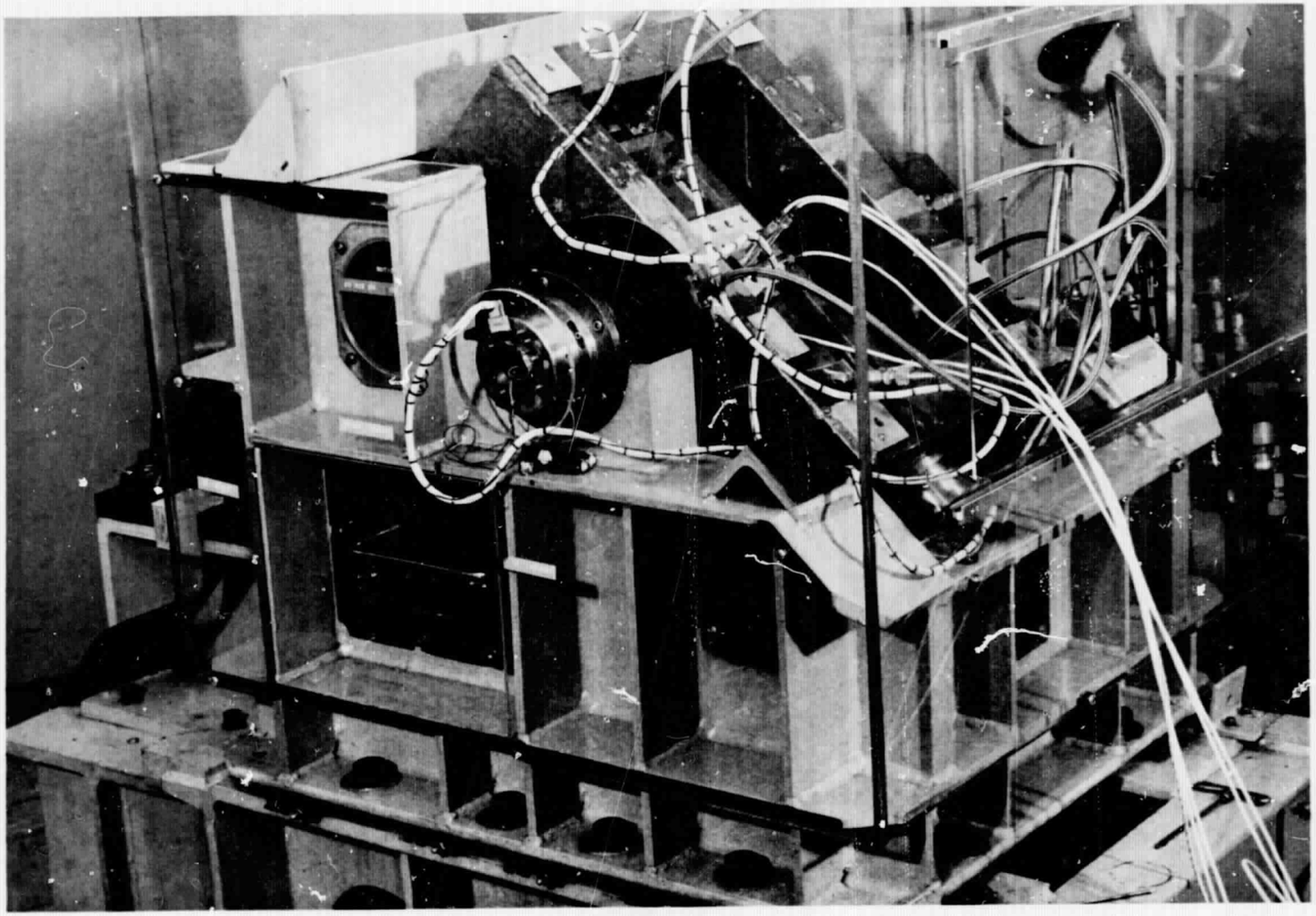

Fig. 7 MIT precision angular vibrator.

High-Speed Touchdown Test

Following the angular vibration tests, each wheel assembly was rate-tested on the Genisco Rate-of-Turn Table to the point of touchdown. Wheel power was monitored during slewing, and the change in wheel power as a function of rate-of-turn input is plotted in Figs. 8 and 9 for the two wheels tested.

Slew-Rate Testing of Wheel 18 BM - 1

Wheel 18 BM - 1 had been subjected to the standard evaluation tests and was to be used for the extended evaluation slew-capability tests when it was noted that the assembly's endshake measurement was below the specification limit. It was felt that this would adversely affect the slew-rate capability. Wheel 18 BM - 3 was substituted as the environmental test wheel. To test this premise, a slew test to the "knee of the curve" (i.e., that slew rate at which the change in wheel running power increases rapidly with a small increase in slew rate, indicating that the rate is just below the touchdown rate for that assembly) was performed on wheel 18 BM - 1 with the following results:

Maximum slew rate before touchdown, initial position:

Clockwise Slew - 9.43 rad/sec

Counterclockwise - 5.44 rad/sec

The wheel running power vs. slew-rate curves for this run are shown in Fig. 10.

Because of the apparent difference in slew-rate capability between the clockwise and counterclockwise rotation of the rate table, it was decided to index the wheel 90° about the SRA position and recheck the slew-rate capability of the wheel. This gave the following results:

Maximum slew rate before touchdown, wheel indexed 90° from initial position about SRA:

Clockwise Slew - 8.97 rad/sec

Counterclockwise - 9.16 rad/sec

The wheel power vs. slew-rate curves for this run are shown in Fig. 11.

Since the slew rate capability appeared to be position-sensitive for this assembly, it was decided to repeat the slew tests indexing the shaft in 15° increments about the SRA to determine if a max/min position existed which could be related to any geometric peculiarity of the assembly (e.g., squareness of sleeve or rotor, etc.).

The wheel was being tested in its sixth incremental test position (i.e., a

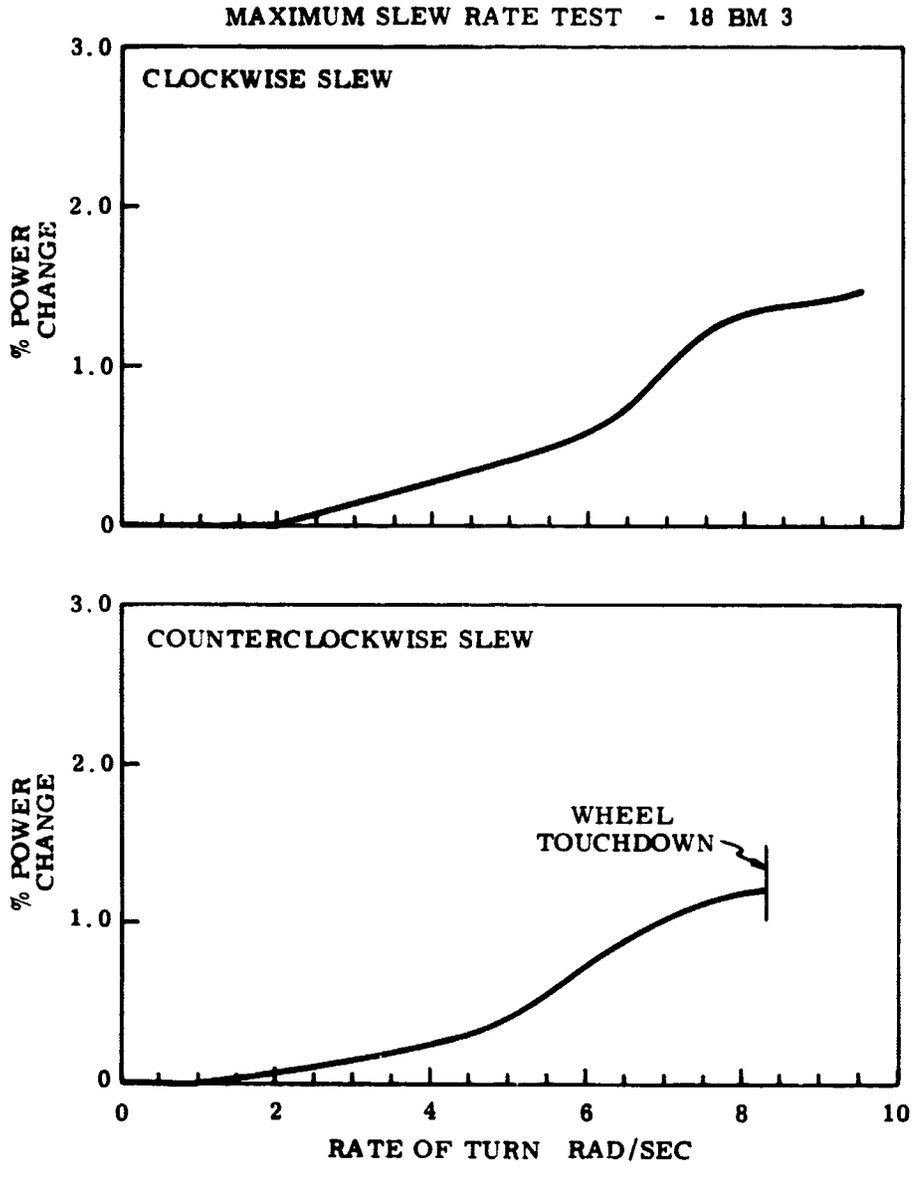

Fig. 8 Change in wheel power as a function of rate input for wheel 18BM-3.

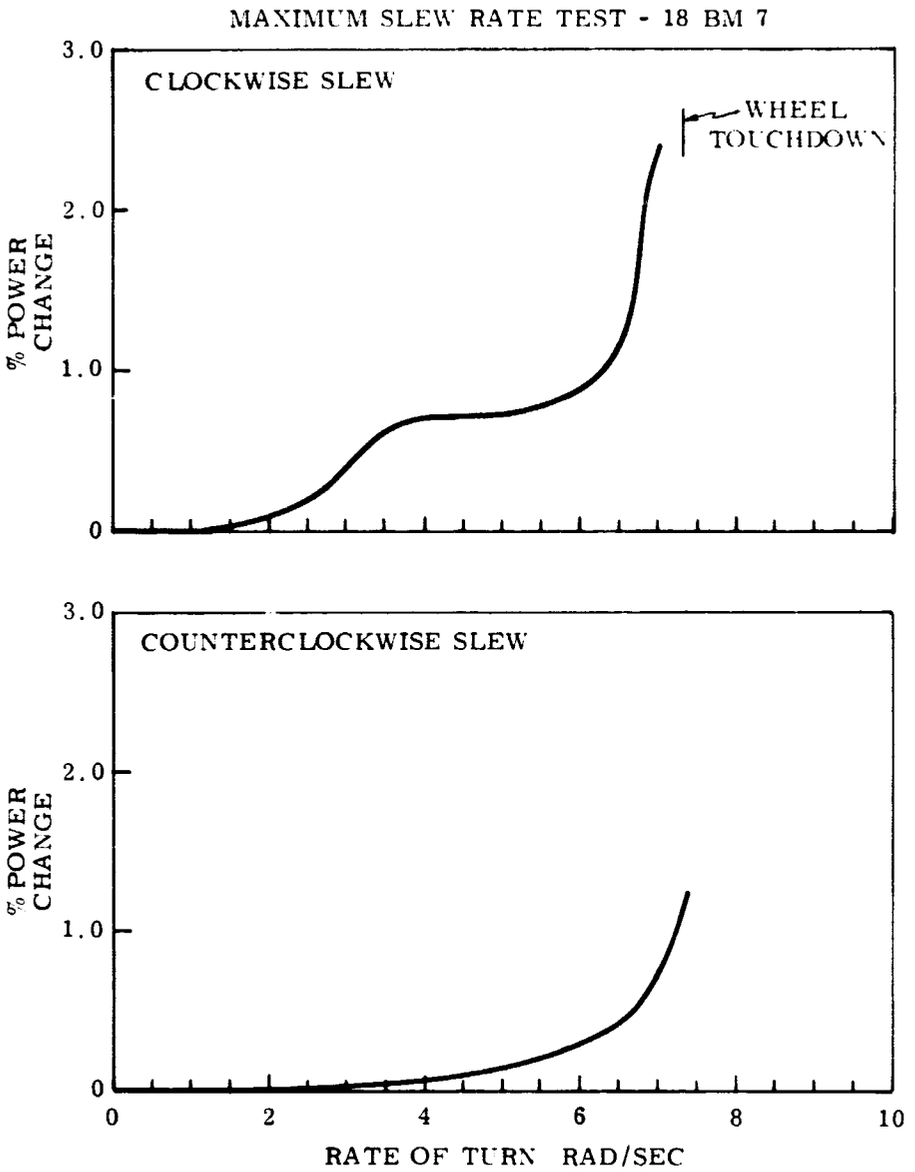

Fig. 9 Change in wheel power as a function of rate input for wheel 18BM-7.

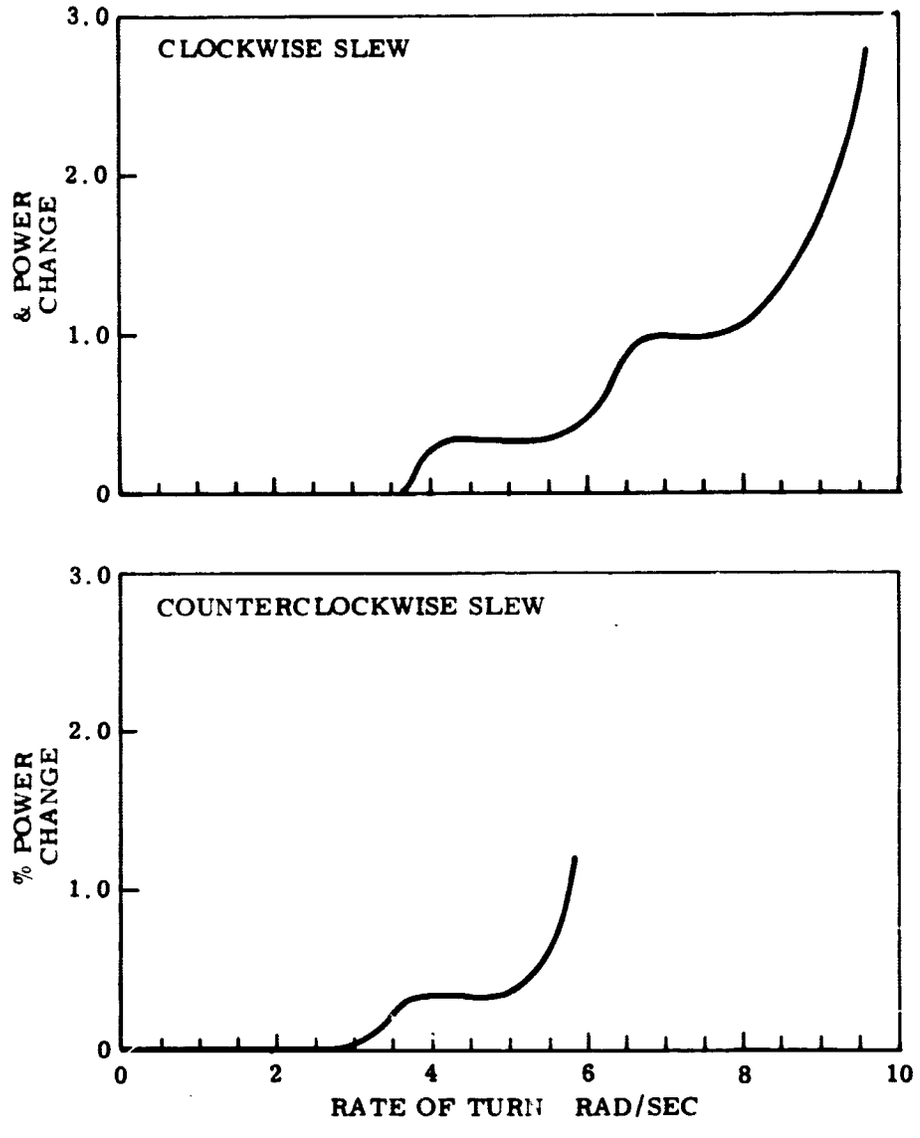

Fig. 10 Change in wheel power as a function of rate input for wheel 18BM-1. Clockwise and counterclockwise slew, initial position.

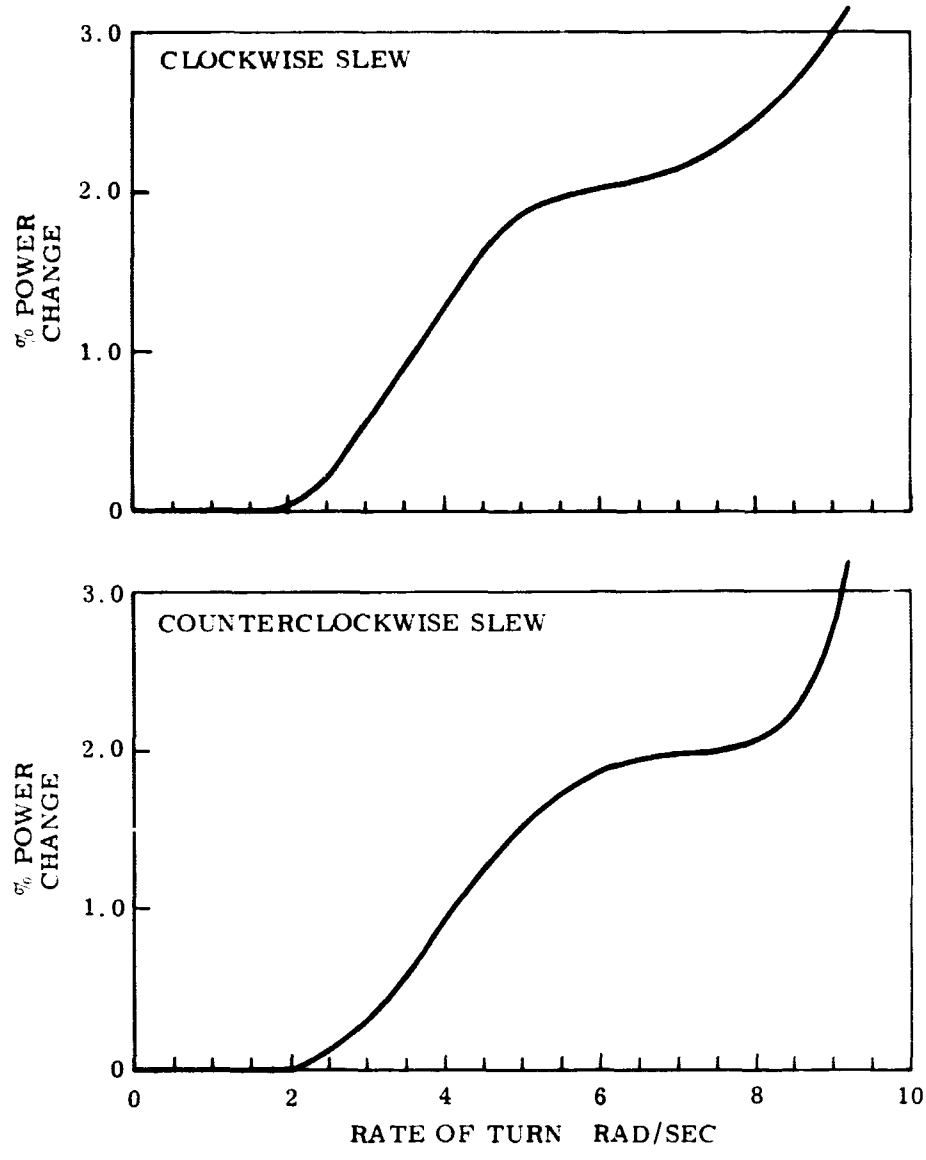

Fig. 11 Change in wheel power as a function of rate input for wheel 18BM-1. Repeat of slew test 90° from initial position, clockwise and counterclockwise slew.

position of 75° rotation about the SRA from the initial position) when it was accidentally bottomed out at a slew rate of 12.6 rad/sec clockwise. Prior to touchdown, the wheel had exhibited a maximum slew-rate capability of 10.8 rad/sec. Although the wheel continued to run following this accidental touchdown, the slew capability of the assembly was reduced to about 1 rad/sec.

Teardown of the wheel revealed that the touchdown had occurred on the journal. However, the mode of failure for this assembly differed from that observed with the AX-1 or Lucalox ceramics previously used. That is, there were no signs of grain-boundary etching in the wear scar as observed with AX-1 or Lucalox. (See Fig. 12.) Rather, the AVCO hot-pressed material exhibited a wear scar resembling a peeling of a layer of material from the surface with no gross subsurface damage apparent.

Following teardown and examination of the wear scar caused by the slew touchdown on this assembly, an inspection of the piece parts was performed to determine if any geometric irregularities contributed to the difference in slew-rate capabilities observed. Inspection revealed that the right thrust face of the rotor was out of square to the bore by 18 microinches. (Spec limit is 10 microinches.) Also the squareness of the journal right end to the OD of the journal was 25 microinches. All other dimensions appeared to be within spec. This lack of squareness of the rotor and journal would certainly account for the "tight" endshake measurement previously measured and could well be the reason for the differences in slew-rate capability observed during clockwise and counterclockwise rotation. Initial inspection of these piece parts had shown them to be within spec. Therefore, it is not known why they now are out-of-spec.

It was also noted that the damage occurred to the journal on the right end, the end which was out of square.

No cause for this dimensional variance could be found, nor could it be determined to what extent it was the cause of the slew-capability variations, nor to what extent it was the result of the high-speed touchdown.

Determination of Slew-Rate Capability

The comparison between the maximum slew-rate test and the low-frequency limits of the angular vibration tests are presented in Table V.

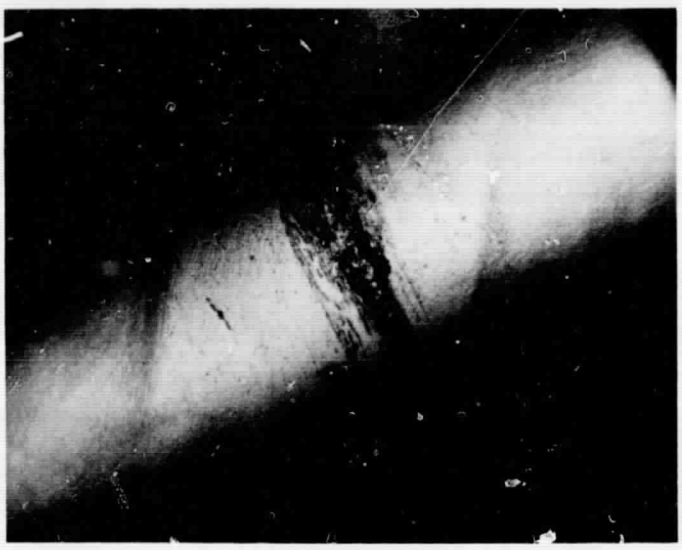

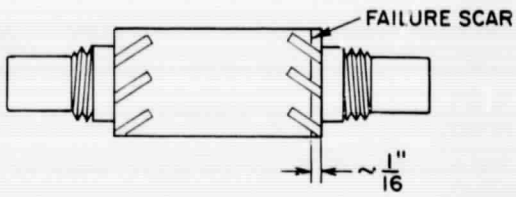

SHAFT AND SLEEVE ASSEMBLY

(a) 50 X

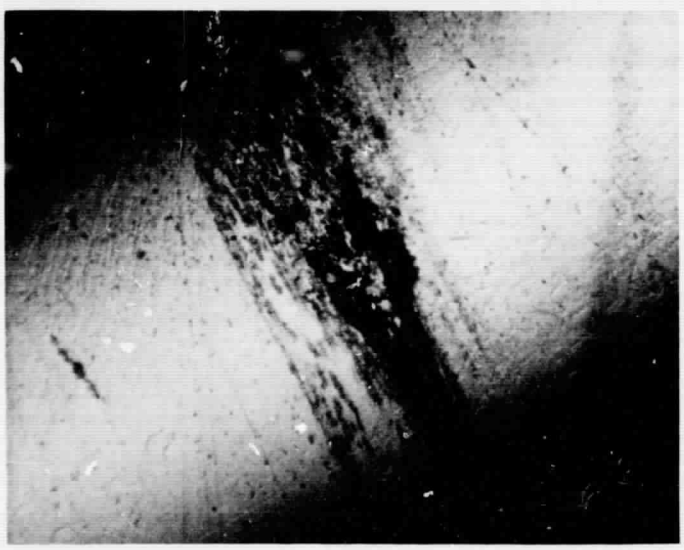

(b) 100 X

Fig. 12a Photomicrographs of failure scar on journal sleeve from wheel 18 BM-1 after slewing to touchdown.

(c) 200 X

Fig. 12b Photomicrograph of failure scar on journal sleeve from wheel 18 BM-1 after slewing to touchdown.

TABLE V

Slew-rate capability determination comparison

Test	Wheel 18 BM-3	Wheel 18 BM-7
Angular Vibration Test on MB C-1050 Torsional Calibrator 20-1800 Hz	7.2 Rad/sec	6.0 Rad/sec
Angular Vibration Test on MIT Precision Angular Vibration 7.5 - 70 Hz	7.7 Rad/sec	6.6 Rad/sec
Maximum Slew Rate, Clockwise	9.5 Rad/sec	7.3 Rad/sec Touchdown
Maximum Slew Rate, Counterclockwise	8.3 Rad/sec Touchdown	7.3 Rad/sec

Figures 5 and 6 show the angular vibration capability for wheels 18 BM-3 and 18 BM-7 in both the MB Torsional Calibrator and the MIT Precision Angular Vibrator tests. Two curves result from each test: one is the response of the rotor about the input axis (as measured by probes #1 #2 and #3 of Fig. 4); the other is the precessional response (i.e., the response normal to the input axis as measured by probe #4, Fig. 4). It is this precessional response, at least for frequencies below 1000 Hz, that provides the limiting slew-rate capability. Were it not for this rotor precession, the wheel would have the rate capability illustrated by input axis response curves.

The values given in Table V represent the limit of rate capability as the angular frequency approaches zero.

One other fact illustrated by these curves is the angular resonance of these wheels. This occurs at 1800 Hz for wheel 18 BM-3, at which point its angular rate capability is reduced to 0.36 rad/sec, and at 1670 Hz for wheel 18 BM-7, at which point the angular rate capability is 0.18 rad/sec.

Table V also lists the maximum slew rates as determined by slewing wheels 18 BM-3 and 18 BM-7 to the "knee of the curve" for one direction of table rotation, then slewing these wheels to touchdown in the opposite direction.

Wheel 18 BM-3, as well as 18 BM-1, was of the AVCO hot-pressed alumina. Wheel 18 BM-7 was made from AVCO hot-pressed alumina with vapor-plated alumina on the bearing surfaces. As was noted, wheel 18 BM-1 had varying rate limits depending upon the shaft position in the fixture, but eventually touched down at 12.6 rad/sec. 18 BM-3 touched down at 8.3 rad/sec., but went as high as 9.5 rad/sec in the opposite direction; 18 BM-7 touchdown at 7.3 rad/sec and went as high as 7.3 rad/sec without touchdown in the opposite direction. Therefore it can be concluded that the rate capability of a wheel as determined by slew testing is affected by the alignment of dimensional deviations in the assembly and that the rate limit, as determined from angular vibration measurements, provides a conservative estimate of the rate capability of the assembly without subjecting it to possible loss due to touchdown.

High-Speed Touchdown Survivability

Wheel 18 BM-3 was slew tested to touchdown in the counterclockwise direction. Immediately following touchdown, the slew rate was reduced to zero, and the wheel restarted when the input rate was removed. Reslewing the wheel indicated that that the rate capability was now reduced to 2.4 rad/sec, whereupon the wheel seized.

As was noted earlier, similar conditions gave similar results for the touchdown failure of wheel 18 BM-1, i.e., following touchdown the apparent rate capability was reduced to about 1 rad/sec.

In testing Wheel 18 BM-7 to touchdown, the rate input was increased following the touchdown, then removed to see if the wheel would start. In this case, however, the wheel failed to restart after the initial touchdown, and teardown revealed that the wheel had seized.

Teardown and examination of these wheels revealed that the failure scars in the AVCO hot-pressed material exhibited a minimum of the grain-boundary etching which had been characteristic of the previously tested aluminas.

Figures 13a and 13b show sections of the failure scar from the journal sleeve of wheel 18 BM-3. Figure 14 shows talysurf traces taken across the damaged area at three positions around the sleeve circumference for the wheel. From these figures it may seem that some grain boundary etching did occur in the damaged region and, though the scar did not extend across the journal grooves, at some points it did reach depths equivalent to the journal groove depths (i.e., 100 microinches).

Figure 15 shows similar talysurf traces taken across the damaged area in the rotor bore of wheel 18 BM-3, taken at three positions 120° apart. These traces show the effect of material build-up in the scar region following the wheel touchdown, as evidenced by an actual transfer of material from one member to the other and suggesting that extreme temperatures do indeed develop at the point of touchdown.

Figure 16 shows the failure scar from the journal sleeve of wheel 18 BM-7. Here it may be seen that more grain-boundary etching did occur in the damaged area, although the resulting scar was not as severe as the one in wheel 18 BM-3.

The parts for Wheel 18 BM-7 were polished to remove any loose particles from the scored region, and the wheel was re-assembled and rate tested again. As was expected, the rate capability was only 1.5 rad/sec clockwise and 2.6 rad/sec counterclockwise, indicating that the effective foreshortening of the journal, due to the scoring, does in fact decrease the rate capability.

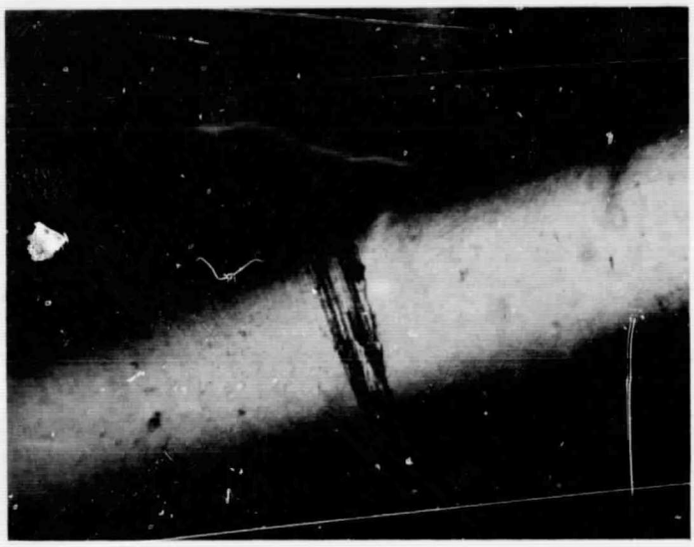

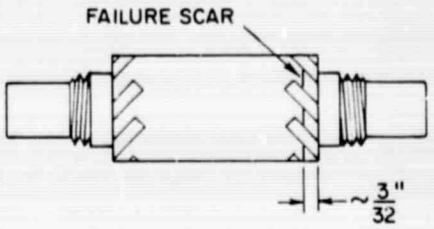

SHAFT AND SLEEVE ASSEMBLY

(a) 50 X Photomicrograph of failure scar extending into journal groove.

(b) 50 X Photomicrograph of failure scar (different region than in a) showing grain-boundary etching.

Fig. 13 Failure scars on wheel 18 BM-3 journal after slewing to touchdown.

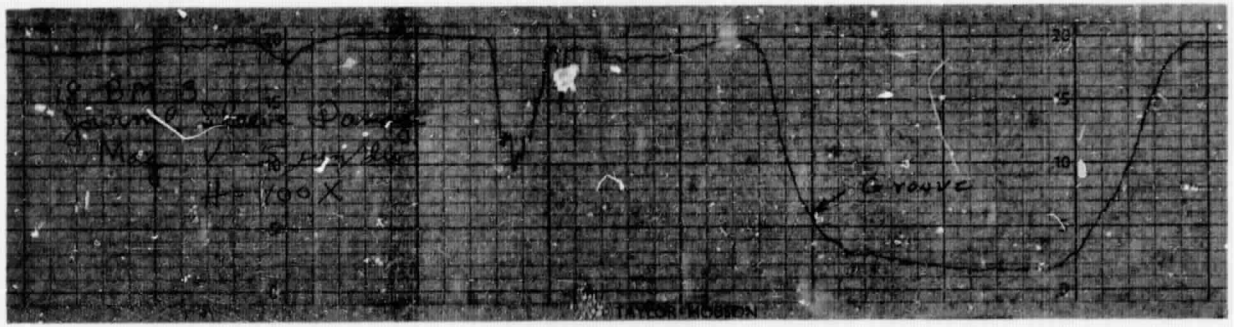

(a) 0^{o} Position

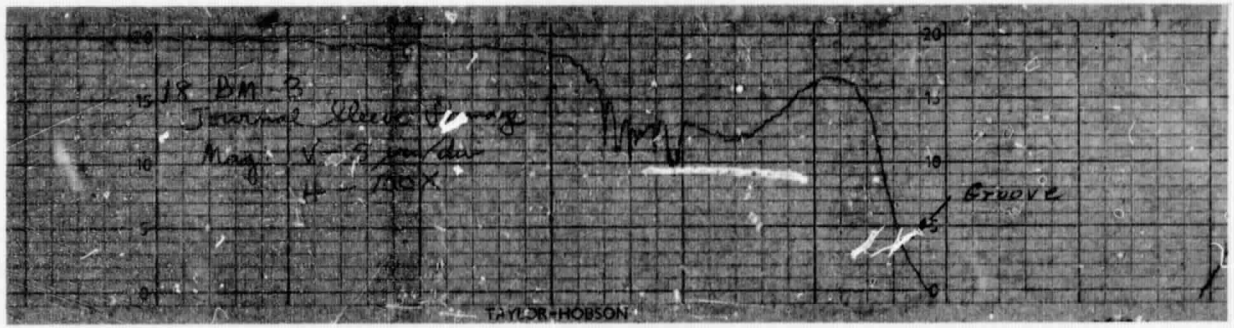

(b) 120^{o} Position

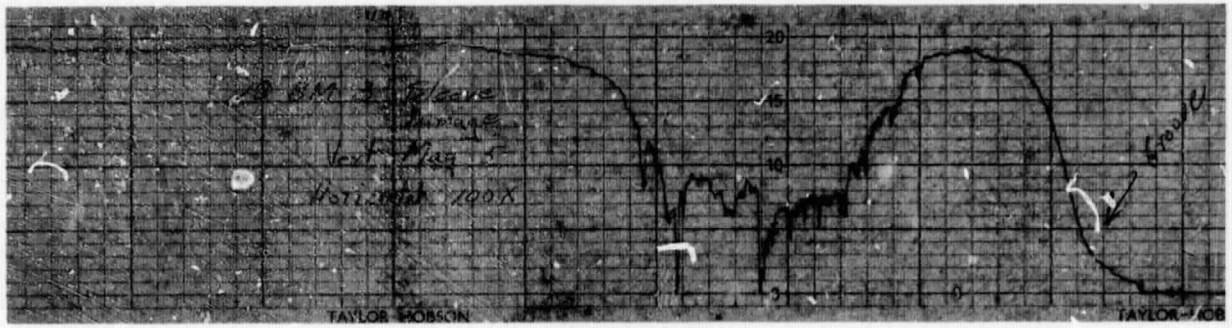

(c) 240^{o} Position

Fig. 14 Talysurf traces taken across failure scar on journal of wheel 18 BM-3 following slewing to touchdown.

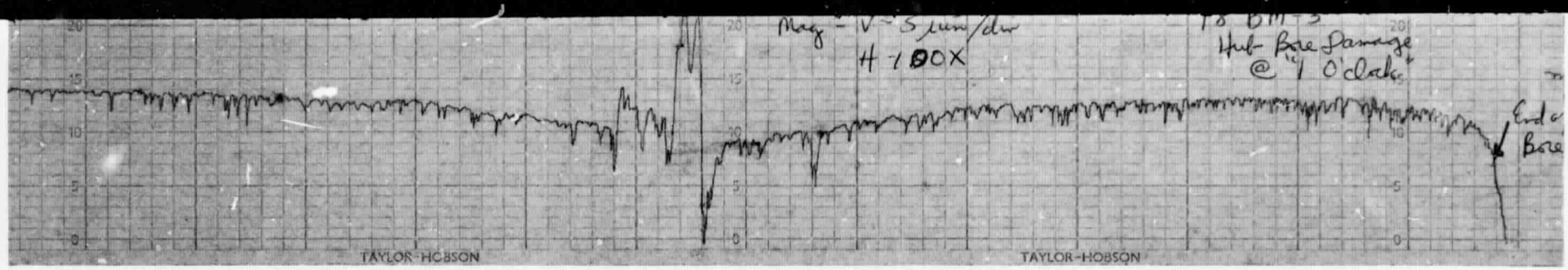

(a) "1 o'clock" position

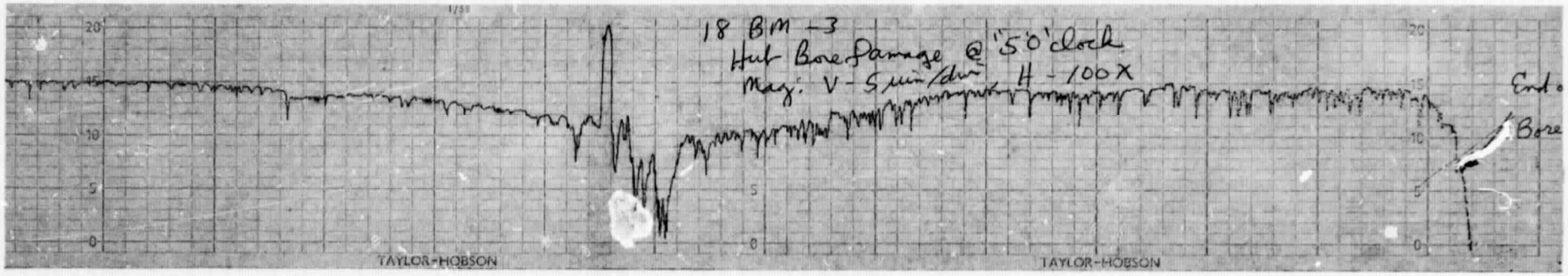

(b) "5 o' clock" position

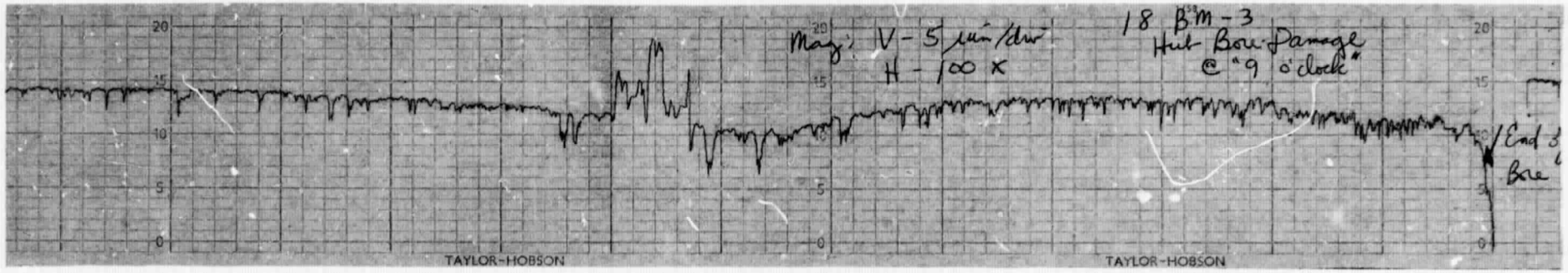

(c) "9 o'clock" position

Fig. 15 Talysurf traces taken across failure scar in rotor bore of wheel 18 BM-3 following slewing to touchdown.

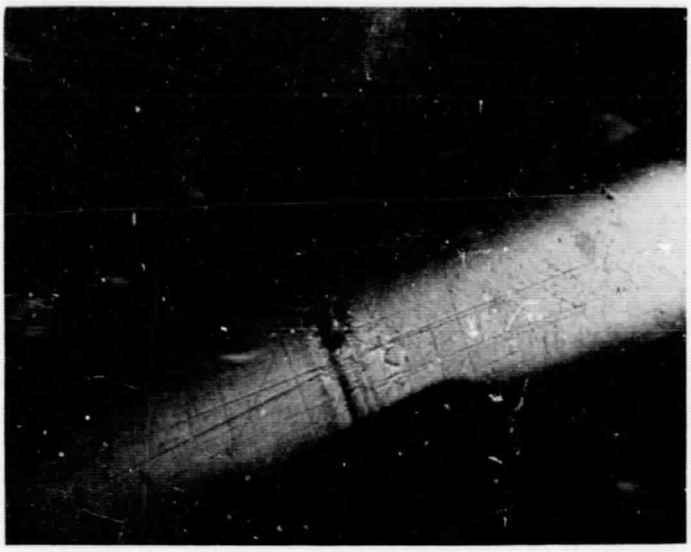

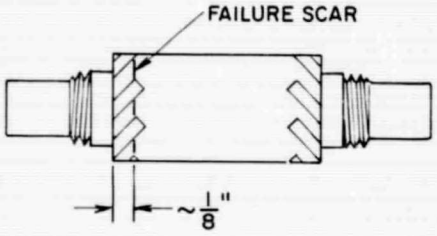

SHAFT AND SLEEVE ASSEMBLY

(a) 50 X Photomicrograph of failure scar.

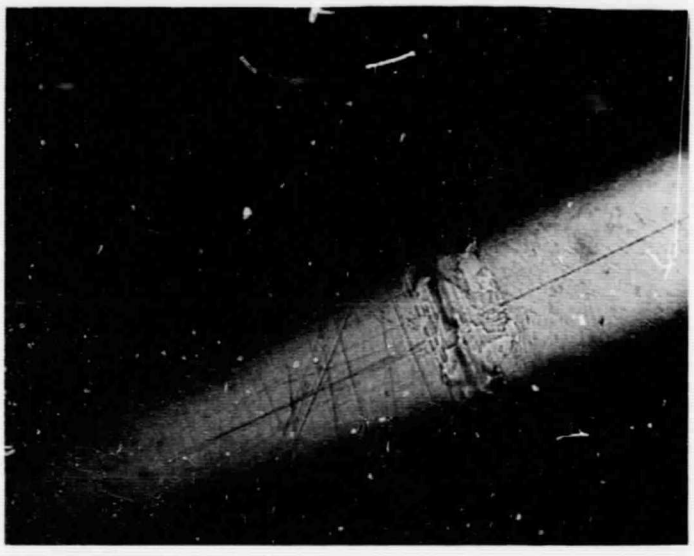

(b) 50 X Photomicrograph of failure scar (different region than in a) showing grain-boundary etching.

Fig. 16 Failure scars on wheel 18 BM-7 journal after slewing to touchdown.

CHAPTER VI

CONCLUSIONS AND RECOMMENDATIONS

1. Materials Development and Evaluation

One of the prime objectives of this program was the development of a suitable gas bearing material. Towards the end, a suitable procurement specification describing the high purity vacuum hot-pressed alumina ceramic has been prepared. (See Appendix III.)

Though no equivalent specification was written for the vapor coating, the characteristics of this coating are controlled by (a) the characteristic of the base material being coated, and (b) the processes itself. (See References 1, 4, 5, and 6 for additional information on the plating process.) Since the vapor coating duplicates the grain structure of the substrate, at least for the first 0.006 inches of coating thickness (See Appendix I), the same specifications for the substrate material should also apply for the vapor coating.

The fine grain-size hot-pressed aluminum oxide, both with and without vapor-coating of the same material, proved to be superior to the previously tested aluminas, both from the standpoints of achievable surface finish and improved strength.

The fine grain-size material also results in improved machinability of thrust pads as seen in Fig. 17a, b, and c. Figure 17a represents Whipple grooves ultrasonically machined in a medium grain-size cold pressed and sintered alumina, such as AX-1 or LUCALOX; Fig. 17b and 17c show the results of the same machining process used to generate Whipple grooves in vapor plated alumina and the AVCO hot-pressed alumina (without plating), respectively. Here it is evident that the fine grain-size and uniformity of the material has greatly contributed to a finer definition of the groove edges and to a much smoother surface at the base of the groove.

Either variety can be recommended for gas-bearing application as an improvement over the cold-pressed and sintered aluminas presently specified. The difficulties encountered in machining the vapor-plated blanks to the appropriate prefinish dimensions were of a one-time nature which could be anticipated on any future material processing.

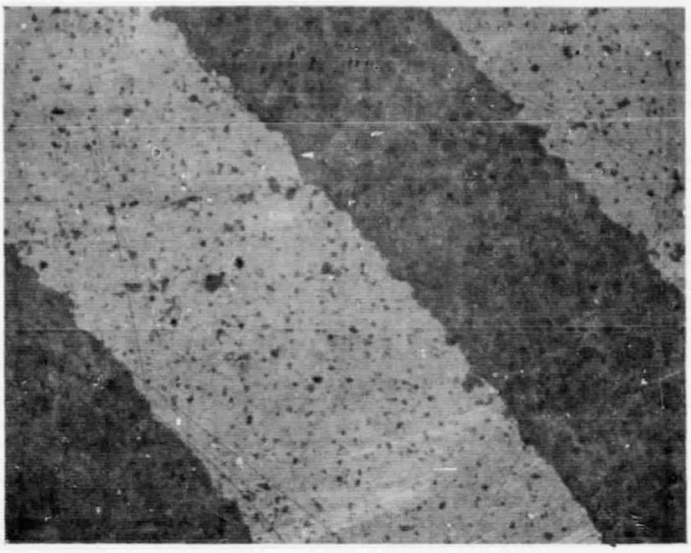

Fig. 17a Whipple grooves machined in medium grained alumina by ultrasonic machining technique (100 X).

Fig. 17b Whipple grooves machined in vapor plated alumina by ultrasonic machine technique (100 X).

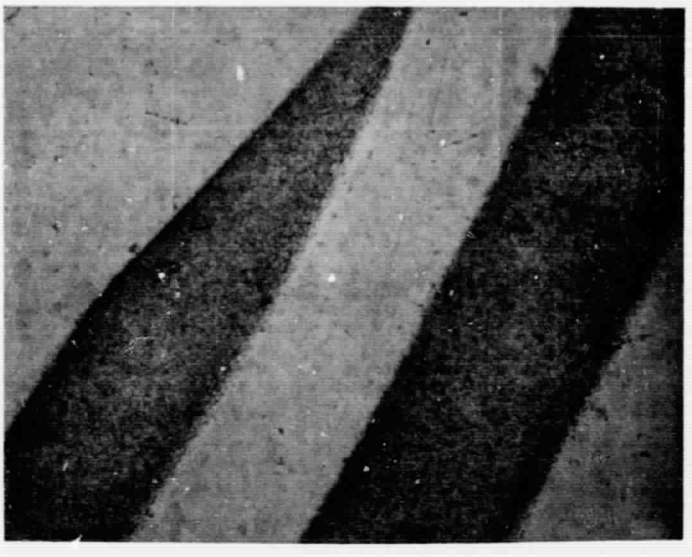

Fig. 17c Whipple grooves machined in AVCO hot-pressed alumina by ultrasonic machining technique (100 X).

2. Extended Start-Stop Capability

The extended start-stop test results indicate that the AVCO hot-pressed alumina offers a threefold improvement over conventional gas-bearing alumina assemblies. With the addition of the vapor-deposited coating on the AVCO alumina as a substrate, it is possible to increase this start-stop capability twentyfold.

Two ever-present factors which influence this capability, of course, are cleanliness and the use of boundary lubricants. Every precaution was taken in these assemblies to insure adequate cleanliness, with strict adherance to conventional gas-bearing cleaning procedure (as called for in the 18 IRIG Mod B Assembly Procedure IC-1399). However, improvements in this process should be investigated.

Proposed Cleanliness Program

A program to investigate alternate cleaning methods should be initiated, first to reduce the processing time and secondly to prepare the surface for better microlubrication adherence. The approach which appears most appealing is cleaning by an ionic bombardment technique. Not only would this approach reduce the time needed for cleaning a set of bearing parts from 4-6 hours to approximately 15 minutes, but it would also remove contamination more effectively, since this process can attack adsorbed as well as surface layers of contaminant molecules.

In conjunction with the above program some criteria for cleanliness must be established. An approach which should meet these needs is the radiotracer method used in studying thin films. In this technique the microlubricant, tagged with a radioactive tracer, is used as the contaminate detector source. A pilot program could be set up with the Health Radiation Center at MIT to check the potentiality of this approach.

Since the radiation counts per unit time are a function of the number of layers of lubricant, the Langmuir Trough method for depositing films of known thickness would need to be established and perfected. Once the proper relationship between radiation counts and layers of microlubricant were established, this procedure could be used not only as a criterion for cleanliness, but also as a means of establishing the number of lubricant monolayers deposited on actual hardware during the building program. It would also act as an excellent quality control device for microlubricant thickness.

The microlubricant used for all of these assemblies was reagent-grade sodium stearate. The methods of preparation and application are specified in Appendix II. It is apparent, however, from friction measurements and start-stop testing of the same wheel following numerous assemblies (including cleanings and microlubrications) that control of the boundary lubricant is difficult to maintain. Therefore this critical area deserves further study.

Proposed Microlubricant Study

A comprehensive microlubrication investigation should be started to establish better application techniques, lubricant performance, and reliability. Alternate microlubricants as well as special atmospheres should be investigated to determine their effect upon initial friction levels, start/stop capability, and wear life. Also, work should be done to determine the melting-point temperature of these lubricants, since values for some of the lubricants under consideration are not available in handbooks and since the melting-point temperature is usually in the range of those temperatures used in temperature cycling and curing of the gyro.

Further testing should include measurements made on assemblies without any microlubricant, in order to establish fully the benefits accrued from the use of boundary lubricants.

It is proposed that the balance of the wheel assemblies remaining in this program be used for continued evaluation studies, including additional extended start-stop testing to build up a larger sampling of data on the behavior of the material combinations in question.

3. Slew Capability

The use of the angular vibrator provides a conservative estimate of the rate capability of a wheel with less chance of endangering the wheel by an unexpected touchdown than that incurred using the rate-of-turn table.

Agreement between the rate capability as determined by the angular vibration tests and that obtained by slewing to touchdown was good, considering the various factors which tend to influence these test results. First, the maximum slew-rate tests were run at 135°F, while the angular vibration tests were run at room temperature. Since rate capability should increase with temperature (as a result of increasing gas viscosity), the results of the maximum slew-rate tests would be somewhat higher than those of the angular vibration tests.

Secondly, in determining the rate capability from the angular vibration tests, a linear response of the wheel is assumed. From sinusoidal linear vibration testing we have found that the bearing becomes stiffer with increased loading. In all likelihood the same results would be true for angular vibration response as well.

Thirdly, the angular vibration capability is assumed to be directly proportional to the measured journal bearing diametrical clearance. Since the accuracy of this measurement is subject to some error, perhaps as much as 10 percent, this will also influence the accuracy of the rate determined from the measurement.

As was noted for the several wheels tested, even the rate capability as determined by slewing on the rate-of-turn table is subject to fluctuation due to geometry variations existing within a given assembly.

4. Touchdown Survivability

None of the 18 IRIG Mod B design wheels tested could survive a high-speed touchdown without catastrophic failure (i.e. either seizing upon initial impact or greatly reduced rate capability following initial touchdown so as to limit severely any ability to withstand additional rate inputs).

With the present design configuration, the 18 IRIG Mod B wheel will touch down on the journal bearing. This mode of touchdown is nearly always catastrophic. One means of preventing this mode of failure is to change the bearing geometry such that a slewing touchdown occurs on the thrust-bearing surfaces instead of on the journal (Appendix D[1]).

Of course, other factors such as power limitations, space or geometry requirements, or other environmental requirements may make such a design change impractical or impossible.

One factor which may be varied to improved the rate capability of the existing design is to increase the gas pressure. The effect upon the slew rate of increasing the pressure of the Neon gas from one to three atmospheres for Wheel 18 BM-7 is given below.

Pressure of Neon Gas	Total Wheel Power (Watts) @ 28 V/ϕ	Slew Rate Capability (rad/sec) As Determined from Angular Vibration Test
1 Atm	4.02	6.0
2 Atm	4.26	6.5
3 Atm	4.38	7.0

This change, of course, does involve an accompanying change in wheel power as also noted in the above table.

An attempt to correlate the point at which touchdown on the journal occurred (i.e., the + SRA or - SRA end of the journal) with direction of slewing showed that no correlation existed. For example, where Wheel 18 BM-1 touched down on the -SRA end for a clockwise slew direction, Wheel 18 BM-7 touchdown occurred on the + SRA end for clockwise slewing, and 18 BM-3 touched down on the - SRA end for counter-clockwise slewing. Examination of several other touchdown failures verified that

the direction of slew rotation at touchdown had no direct relation to where the touchdown would occur.

One further area worthy of investigation for improved high-speed touchdown survivability would be the consideration of other bearing materials. Two materials which possess unique properties in this regard are:

a. Silicon Nitride

Silicon nitride, a material with a hardness of 2700 Knoop and a density of 3.4 gm/cc, might prove a good gas-bearing material for high-speed touchdown conditions, since $Si_3 N_4$ sublimates at 1900°C which is approximately the temperature generated at high-speed touchdown. Due to this sublimation process, the fusion welding and debris which accompanies high-speed touchdown and which is detrimental to the wheel assembly is eliminated. Since the material now available commercially is not of the best quality, work would have to be done to develop a theoretically dense and pure material which could be fabricated into wheel assembly hardware.

b. Boron Carbide

For a number of years boron carbide has been considered one of the prime candidates for gas-bearing use based upon its high hardness and low-density. This high hardness (3000 Knoop versus 2000 Knoop for aluminum oxide) makes it desirable for start/stop and touchdown capabilities where wear is an important factor. Also the low density (2.50 gm/cc versus 3.9 gm/cc for aluminum oxide) makes it possible to concentrate 30% more of the available weight on the inertia rims for increased angular momentum.

In the past the main drawback in working with boron carbide was the poor quality of the commercially available materials which contained undesirable contaminants in the form of free carbon. Better powder preparation and processing techniques have now resulted in materials which is "clean" enough for gyro usage. In addition, recent studies [3] also indicate that boron carbide may also possess desirable wear properties in rubbing against itself.

Therefore, wear tests should be performed, and wheel assemblies should be built from each of these materials for performance testing, start-stop life, and touchdown survivability.

SUMMARY

1. Fine grain size hot-pressed aluminum oxide should be used in place of the cold-pressed and sintered aluminas for future gas-bearing applications.
2. Further improvement in start-stop life is realizable by using the vapor-deposited aluminum oxide coating on the fine grained hot-pressed alumina as a substrate.
3. An improved cleanliness program is desired to reduce processing time and to improved the adherence of boundary lubricants.
4. Further investigation of the nature of the behavior of boundary lubricants is necessary to improve the reliability and the performance of these materials. This work should include a basic determination of the amount of microlubricant present so that adequate quality control can be established.
5. For improvement in touchdown survivability, further investigation should be pursued in the use of other gas-bearing materials, such as silicon nitride and boron carbide.

APPENDIX I

WEAR TESTING OF AVCO HOT PRESSED ALUMINUM OXIDE

Final Report

Prepared by
Lexington Laboratories, Inc.

for

Instrumentation Laboratory
Massachusetts Institute of Technology
Cambridge, Massachusetts

Lexington Laboratories, Inc.
84 SHERMAN STREET
CAMBRIDGE, MASS. 02140
Area Code 617 · 864-5020

FINAL REPORT

Wear Testing of AVCO Hot Pressed Aluminum Oxide

By: H.A. Hobbs, Jr.
R.C. Folweiler

Contract: NAS 9-4576
Subcontract: 349

1.0 INTRODUCTION

The purpose of this subcontract was to test AVCO hot pressed aluminum oxide, with and without a vapor coating, as a gas bearing gyro material. The test capability of the friction and wear apparatus was also expanded to allow tests to be made under high speed (~8,000 RPM) conditions to simulate high speed touchdown failure modes.

The vapor deposition and wear testing were done at Lexington Laboratories, Inc. Initial grinding of the AVCO alumina was done at Quartzite, Inc., of Malden, Mass., and final finishing of the sleeves for wear testing was done by the M.I.T. Instrumentation Laboratory and Westfield Gage Co., Inc. of Westfield, Massachusetts.

2.0 VAPOR DEPOSITED COATING

Coating of fine-grained hot-pressed aluminum oxide was undertaken in an effort to compare this substrate with the results previously obtained on larger grained aluminum oxide. To provide the blanks for coating, the desired parts were machined such that after coating a thickness of approximately 0.002 inches would be removed while a coating of 0.002 inches thick remained. Coatings were applied by the Lexington Laboratories chemical vapor deposition process which has been previously discussed.

In brief, the coating was applied isothermally at a high temperature and provides epitaxial attachment to the surface to be coated. The resultant surface is free of porosity and has low internal strain. There is no tendency for the coating to spall or otherwise flake off. Areas of the blanks that did not require coating were masked to prevent deposition.

We had anticipated that the hot-pressed aluminum oxide might increase in size upon reheating to the temperature used for coating. Testing of a sample piece, however, indicated that there was no change in size and the parts were machined to the desired size based on this information. It was found subsequently that the actual parts did swell, increasing their dimensions by about 1%. This necessitated remachining the various pieces, which were subsequently re-coated. The swelling required, however, only that we re-coat the rotors, since the dimensional change in the smaller journal sleeves were sufficiently small not to affect

the finished part substantially. The rotors were remachined to pre-coating dimensions. At this time, it was observed that two of the rotors contained substantial surface defects in critical places. Two additional rotors were machined from the original block of hot-pressed material to slightly over-sized dimensions. These rotors were heat treated at the coating temperature without coating to allow any dimensional change to occur. Subsequent to heat treatment, an expansion of about 0.5% was observed. These parts were machined to proper pre-coating dimensions and subsequently coated.

3.0 MATERIALS CHARACTERIZATION

The samples tested were made from AVCO hot pressed aluminum oxide. This material had a grain size (Fig. 1a & 1b) of approximately 4 micro meters, and had a grayish cast, due to carbon pickup from the graphite dies during hot pressing. The material had a density of 3.97 gms/cm^3, (100% theoretical density), and the photomicrographs indicated that most of the voids shown were caused during grinding and polishing the sample for wear testing.

The vapor coated AVCO hot pressed sample (Figs. 5 & 6) duplicated the grain structure of the substrate for the first .006 inches of coating thickness. After this thickness of coating is achieved, the anisotropic growth characteristics of aluminum oxide cause growth of large grains with entrapped voids. This problem has been noted in other work [1] Since our coatings amounted to only an 0.006 inch diametral increase, the grain size of the coating essentially duplicates that of the substrate (i.e., roughly 4 micrometers), and the coating is fully dense. The dark spot seen on Figs. 5 & 6 are pullouts resulting from polishing. No deleterious effects are expected from these pullouts.

4.0

The test apparatus was modified to simulate high speed touchdown modes of failure. The modification consisted of adding a high speed (~8,000 RPM) motor and drive train assembly to the current system. The motor was a 1/4 horsepower, 400 cycle motor, and a motor generator converting 60 cycle to 400 cycle was required.

Speed measurements were taken by using a General Radio 1531 "Strobotac." Actual running speed of the high speed apparatus was 7600 RPM.

Testing of journal sleeves under high speed conditions did not significantly increase our understanding of the wear phenomena. Although much heat was generated during short time intervals (10-15 seconds), no catastrophic failures of the journals occurred. Wear patterns generated were the same as patterns observed under the slower testing procedure normally used, but friction coefficients measured were very much higher. Results of the high speed wear testing are included in the tabulated results for the slow speed friction and wear testing.

Although the high speed tests did not duplicate the "high speed touchdown" mode of failure in which journal and plate weld together and breakoff, several factors about the high speeds should be noted. Very high temperatures were generated within 10 to 15 seconds of testing. According to Rabinowicz,[2] the flash temperature of sliding contact may be calculated empirically using the formula

$$\theta_m = \frac{9400 f_\gamma v}{J(k_1+k_2)}$$

where f is the friction force, γ is the surface energy, v is the sliding velocity, J the mechanical equivalent of heat, and k_1 and k_2 the thermal conductivities of the contacting materials.

Using our test conditions of 7600 RPM (630 ft/sec for a 3/8" diameter rod) and a measured friction coefficient of 0.37, the friction generated amounts to 8,250 watts per square inch. Substituting values for the surface energy (900 dynes/cm) and thermal conductivity (.02 cal/sec - °C - cm^2/cm) of aluminum oxide into the formula given by Rabinowicz, the flash temperature per unit velocity (θ/v, °C/cm/sec) is approximately 0.75, or for a velocity of 630 ft/sec (~1,500 cm/sec), 1125°C as the temperature achieved during sliding contact.

Thus, although actual temperatures at contact were not measured, it seems possible to generate large temperatures and large quantities of energy during high speed runs with sliding contact between the rotating sleeve and the contact slides.

5.0 TEST CONDITIONS AND RESULTS

All tests were run in the wear testing apparatus designed and built previously.[3] The tests were run in a dry helium atmosphere at ambient temperature (75°F ± 5°) and at atmospheric pressure. The dew point of the helium atmosphere was not measured. Samples were cleaned in isopropyl alcohol.

Tests were run at 645 RPM and a load of 0.40 lbs. The slider consisted of a 1/8 inch diameter ground rod of AVCO hot pressed alumina. The results of the tests are tabulated in Table I for both the vapor coated and the plain AVCO hot pressed alumina samples. These results are the average of a diminishing number of test points, and the data are shown graphically with the spread in Fig. 8.

From the results, it can be observed that the vapor coated AVCO hot pressed alumina sample outperformed any sample tested so far. No wear was visible after two hours of continuous running. Previous vapor coated specimens showed wear after 16 minutes. The uncoated AVCO hot pressed alumina showed a wear track after 16 minutes (Fig. 2) which increased in size (Figs. 3 & 4) as running time was increased.

High speed runs did not produce any unusual results and were limited to short times because the coefficient of friction went up and off-scale quite rapidly. Failure modes observed in journal assemblies could not be duplicated by the increased rotational speed of our system. The high speed tests did produce large quantities of energy which had to be dissipated, and an empirical calculation showed the flash temperature at the point of contact to be approximately 1125°C.

6.0 DISCUSSION OF RESULTS AND RECOMMENDATIONS FOR FUTURE WORK

Based on the tests performed, the best material tested for wear resistance is AVCO hot pressed alumina with a Lexington Laboratories, Inc. chemically vapor deposited alumina surface coating. AVCO hot pressed alumina performed, in terms of wear resistance, as well as previously tested vapor coated Greenfield AX-1 alumina. The improved performance of AVCO material over materials such as Greenfield AX-1 and Lucalox should be due to two factors: 1) The much finer grain size of the AVCO material (4 micro meters) compared to Greenfield AX-1 (30 micro meters average size) and Lucalox (48 micro meter average grain size) and 2) the higher density of the hot pressed material (100% density) versus roughly 99% for Lucalox and 97% for Greenfield AX-1.

The grain size factor should be the predominant one in the improved performance of vapor coated AVCO material over vapor coated AX-1 alumina. Although the surface was not as good optically on the vapor coated AVCO specimen compared to the vapor coated AX-1 (compare Fig. 5 with Fig. 7), it would appear that the quality of the surface is good enough for our tests to give meaningful test results.

From the limited high speed tests performed, it appears as if more modifications of the apparatus are necessary to perform meaningful tests. Although we do not consider the coefficient of friction to be of critical importance during slow speed testing insofar as determining wear resistance, the fact that during high speed testing the value rapidly exceeded and could not be measured with the load transducers used previously could be significant. Modification of the load and friction

measuring devices to cover a wider range of value could be accomplished.

For future work, we advocate the use of AVCO hot pressed alumina with Lexington Laboratories, Inc. chemically vapor deposited surface coating of alumina for wear resistance. Experiments on such materials with lubricants to reduce the coefficient of friction should be performed if values of friction around 0.3 - 0.4 are too high for use. The high speed apparatus should be modified to increase its friction reading capacity, and to increase its speed capabilities to 15,000 - 20,000 RPM to duplicate actual gas bearing gyro assemblies in operation. Methods to measure both the energy and temperatures generated during high speed operation should be investigated.

BIBLIOGRAPHY

(1) Hobbs, Waugh, Kingery, and Terrenzio, 1st Quarterly Report, Contract NOOO19-68-C-0378, "Chemical Vapor Deposition of Aluminum Oxide Ceramic Shapes," 1 June 1968.

(2) Rabinowicz, Friction and Wear of Materials, J. Wiley and Sons, New York, 1965. pp 89-90

(3) Folweiler, Hobbs, and Schaffer, Final Report NAS9-4576, Subcontract 304, 31 October 1966.

TABLE I

Wear Observations and Coefficient of Friction Measurements on AVCO Hot Pressed Alumina With and Without Vapor Coating

Time	Speed(RPM)	Load(lbs)	Coefficient of Friction	Remarks:
I Hot Pressed Alumina				
30 sec.	645	.40	0.18	No wear on journal
1 min.	645	.40	0.19	
2 min.	645	.36	0.25	
4 min.	645	.30	0.24	
8 min.	645	.30	0.25	
16 min.	645	.20	0.28	(Fig 2) Wear scar on journal
32 min.	645	.20	0.28	(Fig 3) Larger wear scar on journal
2 hrs.	645	.28	0.26	(Fig 4) Fairly wide scar on journal
10 sec.	7600	.41	0.80	Wear scar on journal
II Vapor Coated Hot Pressed Alumina				
30 sec.	645	.40	0.20	
1 min.	645	.40	0.22	
2 min.	645	.40	0.22	
4 min.	645	.40	0.17	
8 min.	645	.40	0.25	
16 min.	645	.41	0.26	
32 min.	645	.40	0.34	
2 hrs.	645	.41	0.36	(Fig.6) No wear on journal
30 sec.	7600	.41	0.60	No wear on journal

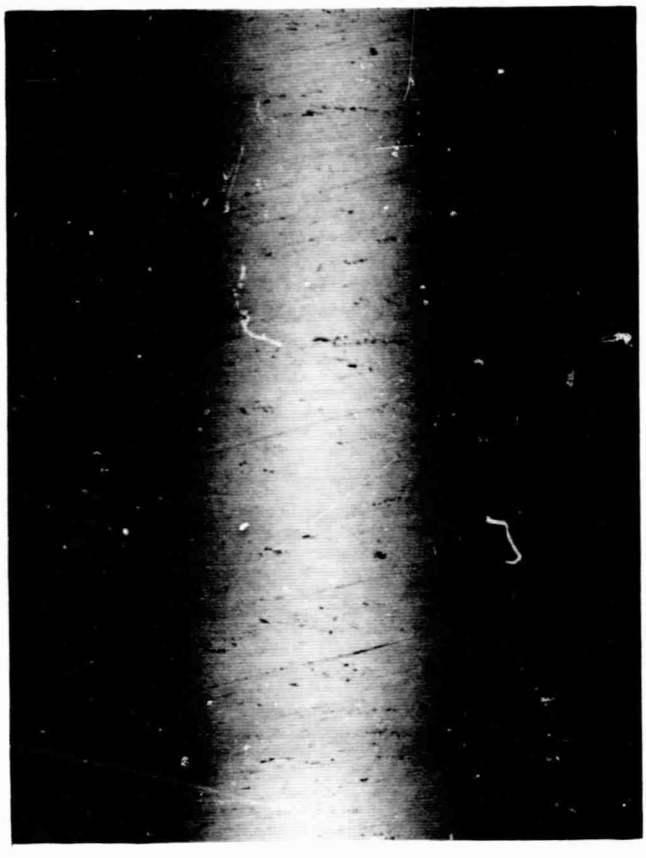

Fig. 1a Hot Pressed AVCO Alumina 66.5X.

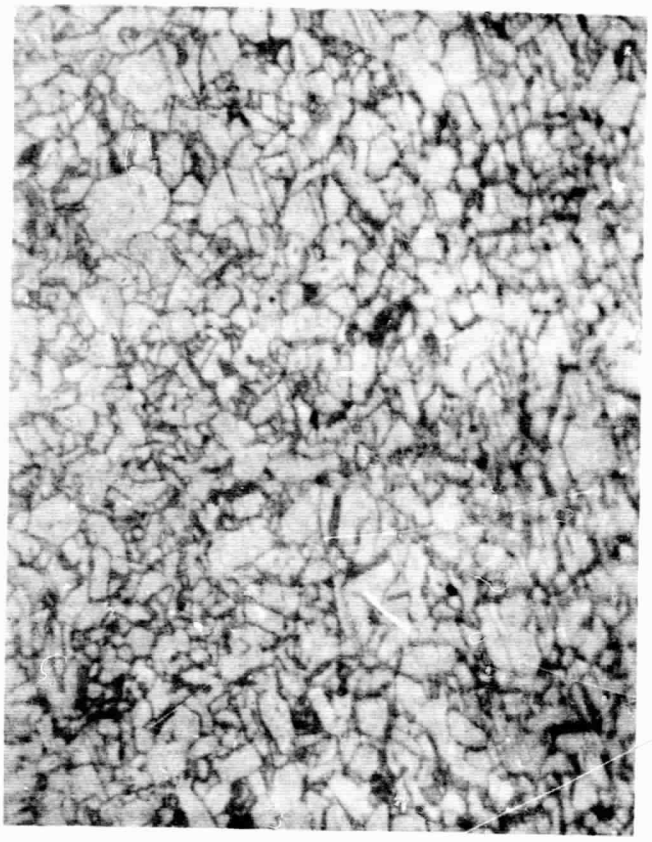

Fig. 1b Hot Pressed AVCO Alumina 532X - Etched.

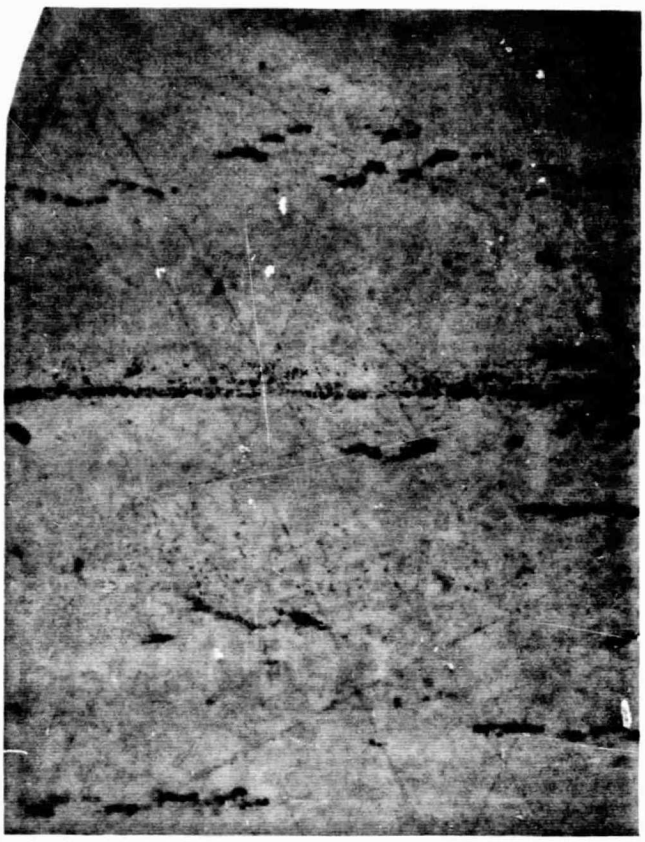

Fig. 2 Hot Pressed AVCO Alumina Tested 16 minutes 266X.

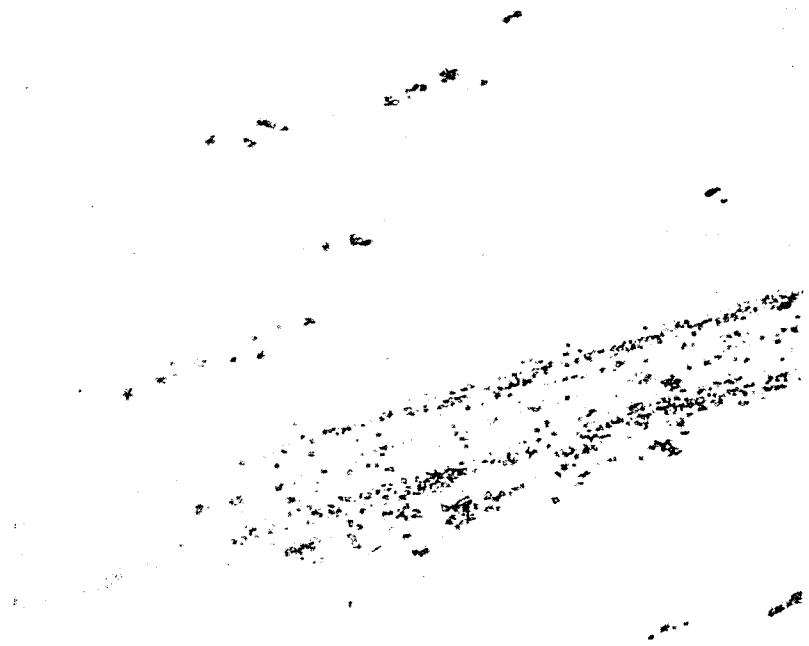

Fig. 3 Hot Pressed AVCO Alumina Tested 32 minutes 266X.

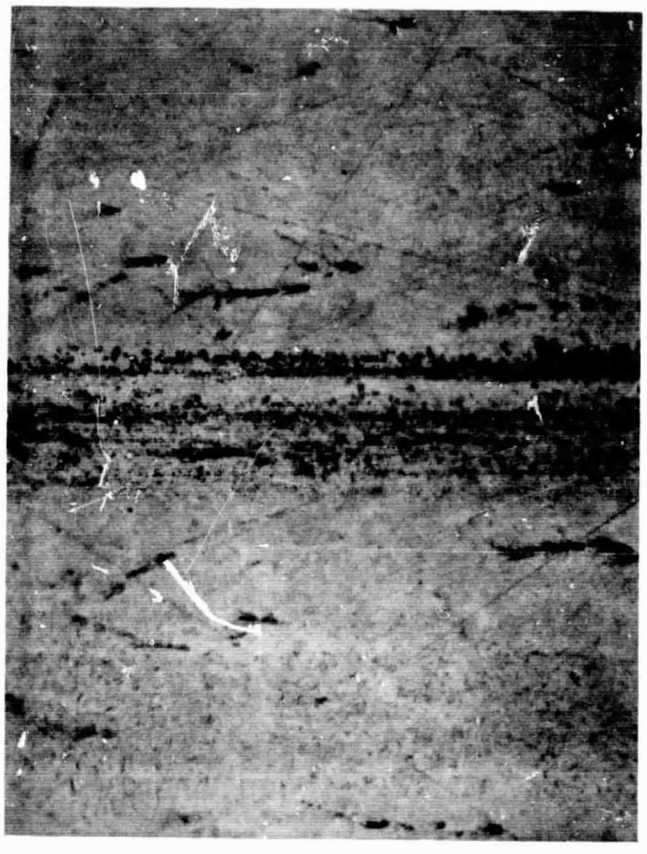

Fig. 4 Hot Pressed AVCO Alumina Tested 2 hours 266X.

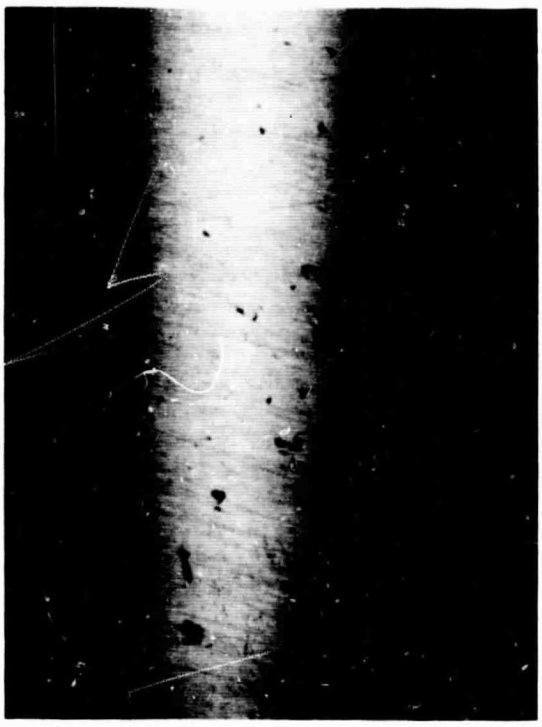

Fig. 5 Vapor Coated Hot Pressed AVCO Alumina 50X.

Fig. 6 Vapor Coated Hot Pressed AVCO Alumina Tested 2 hours 66.5X.

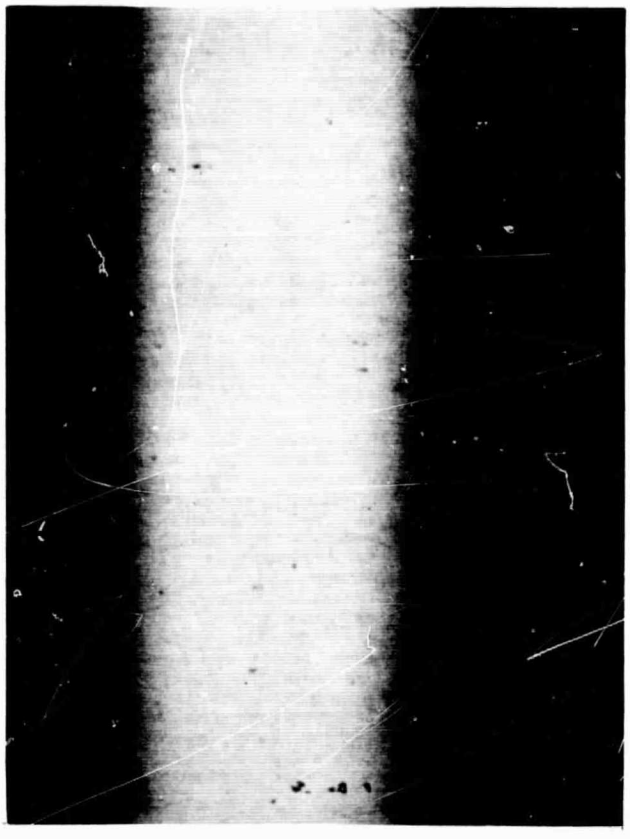

Fig. 7 Vapor Coated Greenfield AX-1 Alumina 66.5X.

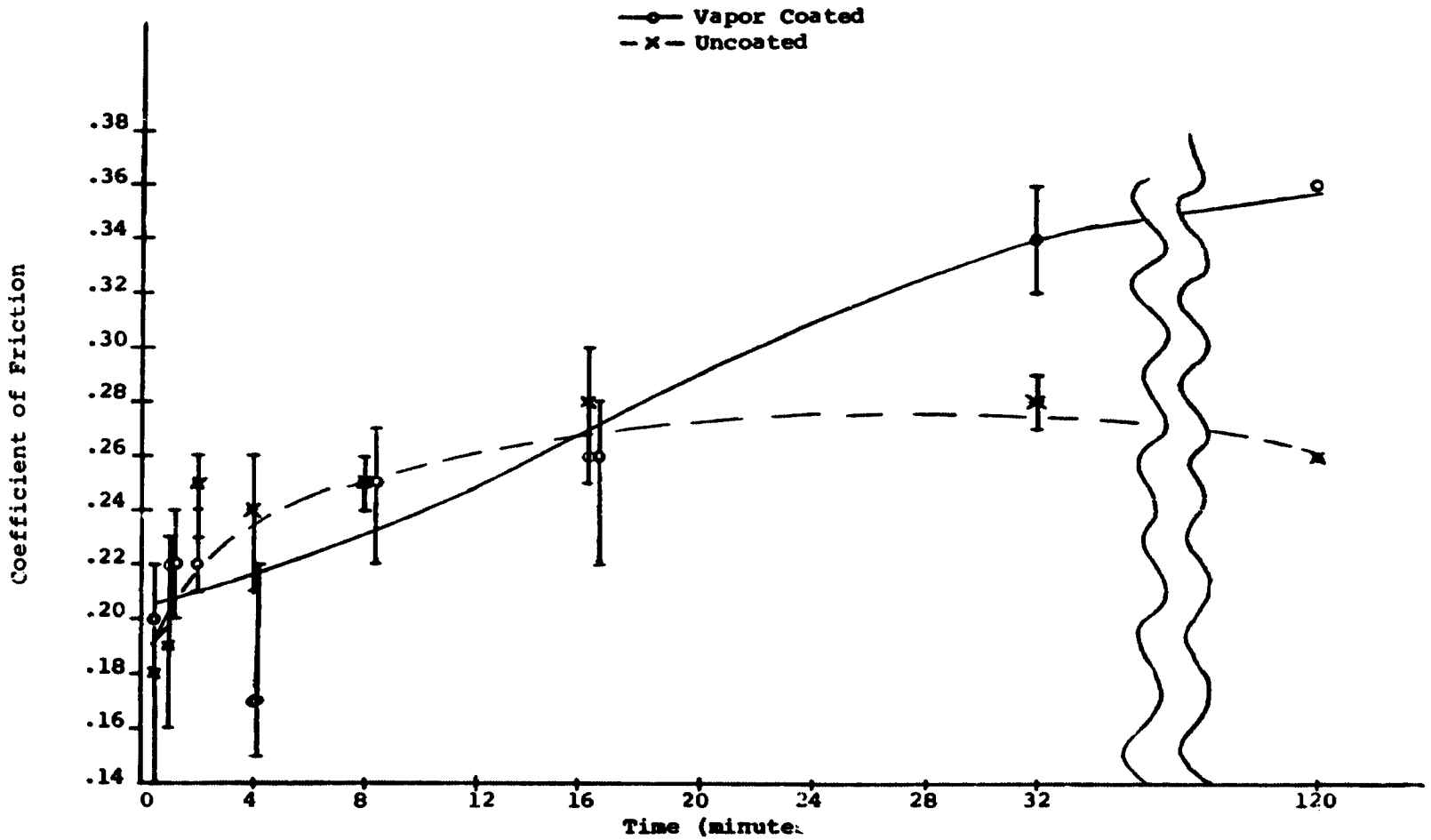

Fig. 8 Coefficient of Friction vs. Time.

ADDENDUM

Answers to Questions from NASA/MSC

1. The comments about wear are qualitative; were quantitative measurements made?

   No quantitative wear measurements were made.

2. What is the coefficient of friction to time zero?

   The tests are run in a manner to establish a kinetic coefficient of friction; thus, a coefficient of friction to time zero, or static coefficient of friction, cannot be established by these tests.

3. The tests on the vapor coated samples are characterized in Table I by higher loads and higher coefficients of friction but less or no wear. On the uncoated samples loads are varied inconsistently. If no correlations exist, how are valid conclusions possible?

   The test was designed to measure wear on samples in sliding contact, and to measure the coefficient of friction during such runs. That no direct and obvious correlation between these two phenomena can be established does not detract from the validity of such tests. We are unaware of any equation which relates the amount of wear, either qualitatively or quantitatively with the measured coefficient of friction. It has been our contention that the coefficient of friction only characterizes the amount of energy necessary to maintain the operation of a system, and in no way determines the wear characteristics of such a system during operation.

APPENDIX II

GAS-BEARING MICROLUBRICATION PROCEDURE

APPENDIX II

GAS-BEARING MICROLUBRICATION PROCEDURE

1. Preparation of Microlubricant

Before cleaning and assembling gas bearing wheel parts, prepare Sodium Stearate microlubricant as follows:

1.1 Into a clean glass beaker pour 500 milliliters of Benzene (Reagent Grade) 500 milliliters of Isopropyl Alcohol (Reagent Grade) and 5 teaspoons full of Sodium Stearate (Reagent Grade). Mix for 1 hour on a Pyro-Magnestir.

1.2 Let the excess Sodium Stearate settle by allowing mixture to stand for 8 hours.

1.3 Pour off the saturated Benzene - alcohol mixture into a clean stoppered bottle and save it for subsequent parts of the microlubrication.

2 Cleaning Procedure

2.1 Cleaning (Rotor)

2.1.1 Scrub each bearing surface with a stiff nylon brush and trichlorethylene before placing in cleaner. Wash rotor in 4 baths of trichloroethylene at 3 minutes each. Scrub the rotor bearing surfaces with a stiff nylon brush and Alconox solution. Rinse part in deionized water 6 times and check for water break. Place part in beaker filled with ethyl alcohol and place in dessicator. Pump down to 25 mm of mercury or less and hold this vacuum for at least 10 minutes to remove any water which may have deposited in gaps or voids. Wash rotor in ultrasonic cleaner in 4 baths of ethyl alcohol at 3 minutes each; vacuum the excess alcohol from the part with a vacuum tip in a Blickman Cabinet and bake out hub assembly for 1/2 hour using the following prodedure:

2.1.2 Place each part in a clean covered glass container and place container over the 100-watt light source in the Blickman Assembly Cabinet with the light Variac set at 75 volts (140° - 145°F). Let container stand at least 1/2 hour to allow parts to dry thoroughly. Provide some means of venting moisture to prevent condensation from forming on inside of the container.

The vacuum tip connected to a vacuum system has proven successful for this application.

2.2 Cleaning (Nuts and Washer)

2.2.1 Wash in the ultrasonic cleaner in two baths of trichlorethylene. Vacuum the excess trichloroethylene with the vacuum tip in a Blickman Cabinet and bake out parts for 1/2 hour using drying procedure of 2.1.2.

3. Microlubrication

Use the following procedure to microlubricate the end caps and shaft and journal sleeve assembly. Scrub each bearing surface with a stiff nylon brush and trichlorethylene before placing in ultrasonic cleaner. Wash each component in 4 baths of trichloroethylene at 3 minutes each in the ultrasonic cleaner. Scrub bearing surfaces of end-caps and journal sleeve with a stiff nylon brush and Alconox solution. Rinse part in de-ionized water 6 times and check for water break. Place parts in separate beakers filled with ethyl alcohol and place in dessicator. Pump down to 25 mm of mercury or less and hold this vacuum for a least 10 minutes to remove any water which may have deposited in gaps or voids. Wash each component in the ultrasonic cleaner in 4 baths of ethyl alcohol at 3 minutes each, then repeat same procedure except with Benzene. Wash each component in the Sodium Stearate Solution (as prepared in Section 1) for ten minutes in the ultrasonic cleaner. Shake off any excess mixture and place parts in Blickman cabinet for drying.

4. Drying Period

Place each component in a clean covered glass container and place container over 100-watt light source in Blickman Assembly Cabinet with the light Variac set at 75 volts ($140^{\circ}F$ - $145^{\circ}F$). Let container stand at least 1 hour to allow parts to dry thoroughly.

5. Processing

Process each of the stearated components as follows to obtain the proper amount of microlubrication. Wipe off any excess Sodium Stearate with clean lens tissue using several layers of tissue. Immerse the parts in Benzene at room temperature for 15 to 30 seconds. Vacuum the excess Benzene from each part with a suction hose and vacuum tip and bake out each component for 1/2 hour in the Blickman Cabinet, using the procedure described in Section 4.

6. Inspection

Inspect each part under a microscope at 16 x and vacuum surface to remove any foreign particles.

7. Assembly

Assemble components as described in the appropriate assembly procedure specification.

Equipment List

Sodium Stearate (Reagent Grade)
Benzene (Reagent Grade)
Isopropyl Alcohol (Reagent Grade)
Trichlorethylene (Reagent Grade)
Alconox - Alconox Inc., New York 3, N.Y.
Ultrasonic Cleaner
Stiff Nylon Brush
Pyro-Magnestir, Lab Line Equipment Inc.
Vacuum Tip
Blickman Assembly Cabinet
Dessicator - Corning #3118
Stereo Microscope
Friction Force Fixture - MIT/IL D-133470
Holding Fixture - MIT/IL C-135552
Torque Wrench
Ethyl Alcohol

APPENDIX III

PROCUREMENT SPECIFICATION FOR VACUUM HOT-PRESSED HIGH PURITY ALUMINA CERAMIC FOR GAS-BEARING APPLICATIONS

APPENDIX III

PROCUREMENT SPECIFICATION FOR VACUUM HOT-PRESSED HIGH PURITY ALUMINA CERAMIC FOR GAS-BEARING APPLICATIONS

1. General

1.1 Scope: This specification establishes the requirements for the procurement of high purity alumina ceramic (vacuum hot-pressed directly from fine powder or cold-pressed prior to vacuum hot pressing).

2. Applicable Documents:

MIL-D-100	Drawings, engineering and associated lists
OD 36352	Product Quality Requirements
OD 36357	Preparation for Delivery of Parts
MIL-I-6866	Inspection, Penetrant Method of
ASTM-D-116	Method of Testing Vitrified Ceramic
ASTM-C-528	Method of Test for Compressive Strength Ceramic
ASTM-C-372	Method of Test for Linear Thermal Expansion of Fired Whiteware Products by the Dilatometer Method
ASTM-C-408	Method of Test for Thermal Conductivity of Whiteware Ceramics
ASTM-C-373	Method of Test for Water Absorption Bulk Density, Apparent Porosity, and Apparent Specific Gravity
ASTM-E-112	Standard Methods for Estimating the Average Grain Size of Metals
ASTM-C-327	Method of Test for Linear Thermal Expansion of Fired Ceramic Whiteware Material by Interferometric Method

3. Requirements

3.1 General

3.1.1 Interpret drawing in accordance with standards prescribed by MIL-D-1000

3.1.2 Quantity and/or size shall be as specified on the purchase order.

3.2 Design

3.2.1 Compressive Strength: The material shall have a minimum

compressive strength of 300,000 psi when tested in accordance with ASTM standard C-528-63T.

3.2.2 Coefficient of Thermal Expansion: The minimum coefficient of thermal expansion shall be 3.4×10^{-6} in/in^{o}F (68^{o} to 212^{o} F range) when determined in accordance with ASTM Standard C-327 or ASTM standard C-372-56.

3.2.3 Poisson's Ratio: When using the sonic method, Poisson's ratio shall lie between 0.20 and 0.30.

3.2.4 Dielectric Strength: The material shall have a minimum dielectric strength of 230 V/mil when tested in accordance with ASTM standard D-116-63.

3.2.5 Thermal Conductivity: The minimum thermal conductivity shall be 115 BTU/ft^{2}/hr/^{o}F/in. when determined in accordance with ASTM standard C-408-58 or any other method acceptance to the purchaser.

3.2.7 Water Absorption: Water absorption shall be 0.0 percent when determined in accordance with ASTM Standard C-373-56.

3.2.8 Grain Size: The final average grain-size of the material shall not exceed 8 microns when determined in accordance with ASTM STD-E-112.

3.2.9 Hardness: The material shall have a minimum hardness of 1600 on the VPN scale.

3.3 Inspection for Acceptance (minimum requirements)

3.3.1 Purity: The material shall have a maximum of 1.5% impurities (sum of additives and impurities) when determined by difference of impurity elements. Metallics shall have a maximum limit of 2000 ppm and silicon 1000 ppm.

3.3.1.1 In general, the impurity elements shall be those regularly analyzed by spectrographic means. Analyses may be performed on a powder lot basis.

3.3.2 Density: The material shall have a density between 3.963 gm/cc (99.4% theoretical) and 3.987 gm/cc (100% theoretical) determined by using a suitable displacement technique with an analytical balance. Within any one lot, the density must not vary more than ± 0.5% of theoretical (±0.02 gm/cc).

3.3.3 Surface Quality: The material shall be free of cracks or in-

clusions in accordance with specification MIL-I-6866, Type I (Fluoresecent Method) and viewed at a magnification up to 20X. Unless otherwise specified, diffused areas characterized by slight surface discoloration shall be cause for rejection when the largest dimension exceeds 0.015 inch. Pits shall be defined as surface cavities (open and partially closed) and, unless otherwise specified, pits having any dimension in excess of 0.005 inch shall be cause for rejection. Chips shall be defined as edge flaws (open and closed) and, unless otherwise specified, chips having any dimension in excess of 0.015 inch shall be cause for rejection.

3.3.4 Surface Finish: The material shall have the following maximum CLA surface finish when measured on a Talysurf surface measuring instrument with a 0.030 inch cutoff:

	CLA
As Fired	55
Ground	32
Lapped and Polished	4

3.3.5 Mechanical: The material shall conform to the following Ultimate transverse rupture strength at room temperature - 60,000 psi.

The ultimate transverse rupture strength is to be determined by a bend bar whose dimensions are:

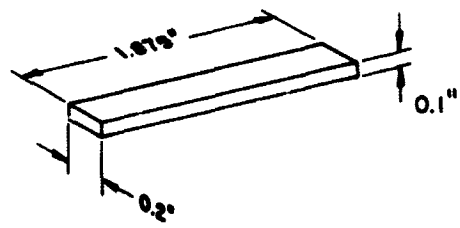

and four-point loading applied as shown below:

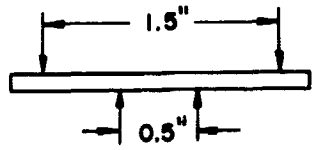

3.3.6 Leak Test: A 1" diameter, 0.030" thick disc shall be checked in a mass spectrograph leak checker. There shall be no measurable leak. (1×10^{-8} cc/sec Helium, maximum).

3.4 Special Conditioning: None

3.5 Quality Assurance Provisions

3.5.1 Suppliers shall conform to quality assurance provisions specified in OD 36352, Class 3.

4. Marking and Packaging

4.1 Preparation for delivery shall be as specified in OD 36357, Code 7.

4.2 Marking: Each shipping and unit container shall be permanently and legibly marked with the manufacturer's name and/or symbol, item name, net contents, lot number, date of manufacture, drawing number, dash number and revision letter.

LIST OF REFERENCES

1. Rowe, Henry H., Jr., The Development of a Gas Bearing Version of the Apollo I Inertial Reference Integrating Gyro, R-571, Instrumentation Laboratory, Massachusetts Institute of Technology, Cambridge, Massachusetts.

2. A Proposal for the Development of Hot-Pressed High-Density Alumina Material Suitable for Gas Bearing Use, prepared by AVCO Space Systems Division, Materials and Engineering Directorate, Lowell, Massachusetts, August 30, 1967.

3. Sellers, P.J., Burnett, P.L., Verneburg, P.L., and Honck, C.L., The Evaluation of B_4C Thrust Pad Surfaces, Summary Report, AVCO Corp. Space Systems Division, Lowell, Massachusetts, September 24, 1968.

4. Rowe, Henry H., Jr., "Measurement and Control of Surface Finish Characteristics of a Gas Bearing Material", Proceedings of the Gyro Spin-Axis Hydrodynamic Bearing Symposium, MIT/IL, Tab 5, December 1966.

5. Schaffer, P., "Vapor-Phase Growth of Alpha Alumina Single Crystals", Journal of the American Ceramic Society, Vol. 48, No. 10, October 1965.

6. Rowe, Henry H., Jr., "An Investigation of Methods to Improve the Wear Resistance of Gas-Bearing Ceramic Materials", Journal of Lubrication Technology, Transactions of the ASME, Vol. 90, Series F. No. 4, October 1968, pp. 829-840.